Ferromagnetism in the one-dimensional Kondo lattice: Mean-field approach via Majorana fermion canonical transformation

Matteo Bazzanella and Johan Nilsson
Department of Physics, University of Gothenburg, 412 96 Gothenburg, Sweden
(Received 4 October 2013; revised manuscript received 11 December 2013; published 15 January 2014)

Using a canonical transformation, it is possible to faithfully represent the Kondo lattice model in terms of Majorana fermions. Studying this representation, we discovered an exact mapping between the Kondo lattice Hamiltonian and a Hamiltonian describing three spinless fermions interacting on a lattice. This alternative form of the Hamiltonian is suitable for an immediate identification of the competing effects that operate in the Kondo lattice model. In particular, a term describing the double-exchange mechanism appears explicitly in the Hamiltonian. We investigate the effectiveness of this three-fermion representation by performing a zero-temperature mean-field study of the phase diagram at different couplings and fillings for the one-dimensional case, focusing on the appearance of ferromagnetism. The solutions show interesting features that agree in many respects with the known numerical and analytical results. In particular, in the ferromagnetic region connected to the solution at zero electron density, we have a quantitative agreement on the value of the "commensurability parameter" discovered in recent density matrix renormalization group (in one dimension) and dynamical mean-field theory (in infinite dimensions) simulations; furthermore, we provide a theoretical justification for it, identifying a symmetry of the Hamiltonian. This ferromagnetic phase is stabilized by the emergence of a spin-selective Kondo insulator, which is described quite conveniently by the three spinless fermions. We discover, however, that such a phase cannot be the correct description for all the ferromagnetic phases of the one-dimensional Kondo lattice model. We found in fact a different ferromagnetic phase at high filling and low couplings. This phase resembles the Ruderman-Kittel-Kasuya-Yosida (RKKY) ferromagnetic phase existing at vanishing filling, but it incorporates much more of the Kondo effect, making it energetically more favorable than the typical spiral (spin ordered) mean-field ground states. We believe that this second phase represents a prototype for the strange ferromagnetic tongue identified by numerical simulations inside the paramagnetic dome. At the end of the work, we also provide a discussion of possible orders different from the ferromagnetic one. In particular, at half-filling, where we obtain as ground state at high coupling the correct Kondo insulating state.

DOI: 10.1103/PhysRevB.89.035121 PACS number(s): 75.30.Mb, 75.10.−b, 75.20.Hr, 71.27.+a

I. INTRODUCTION

The Kondo lattice is one of the most studied models in condensed matter physics [1–4]. The features of this model are approximately explained by the competition between three main phenomena: the coherent formation of Kondo singlets [5–7], the Ruderman-Kittel-Kasuya-Yosida (RKKY) spin-spin effective interaction [8–10], and the double-exchange mechanism [11–13]. The balance between these effects gives rise to highly nontrivial physics that is not easily described keeping the impurity spin and conduction electron degrees of freedom strictly separated. As a consequence, the phase diagram of the Kondo lattice model (KLM) is quite fascinating: by changing only two parameters (the Kondo coupling and the density of the conduction electrons), many different classes of ground states can be explored [1–4]. The KLM can therefore be used as the model Hamiltonian for many interesting systems, such as heavy-fermion compounds [14–16] and Kondo insulators [1,17–21]. It is also believed that many of the currently most studied systems (both by numerical and experimental means), for example, actinide compounds and perovskities [1–4], can be effectively described by the KLM. The existence in the KLM of superconductivity generated by spin fluctuations has also been a source of debate and has recently been addressed by new numerical studies [22,23] that suggested the presence of this mechanism in the Kondo-Heisenberg model.

Unfortunately, few exact solutions of this model are available, and typically only limited regions of the phase diagram can be successfully described by analytical tools. The problems are of course created by the interaction between the conduction electrons and the impurity spins that causes the entanglement [24] of these two quantum degrees of freedom. This poses formal problems and raises profound questions: the former are due to the different operator algebras describing the conduction electrons and the impurity spins that cannot be treated on the same footing; the latter are related to the role of the impurity spins and their debated contribution to the Fermi volume [25].

In some particular limits, the one-dimensional Hamiltonian can be studied analytically. For example, some exact results exist at half [1,17–21] and infinitesimal [26] filling for every value of the Kondo coupling, or at infinite [27] and high [28] Kondo coupling for every value of the filling. Moreover, the low-energy properties of the system can be solved exactly for weak Kondo couplings, making use of bosonization techniques [17,29–31]. However, to explore larger regions of the phase diagram, only numerical methods [1,32–35] can be applied. A standard approach, common to many numerical and analytical studies, is to start from the analysis of the Anderson lattice model and strongly enforce unit occupancy of the f-impurity states. This generates a constraint on the local number of the f electrons that if fulfilled exactly, implies the freezing of their charge degree of freedom, transforming effectively the f electrons into impurity spins [7,15]. Such an approach to the problem relies on the fact that the Kondo lattice model can be seen as the effective low-energy description of the

symmetric Anderson lattice model [36–38], if the hybridization and the confinement potential are appropriately sent to infinity, as prescribed by the Schrieffer-Wolff transformation [39]. The positive aspect of this approach is that all the excitations of the system are fermionic; the constraint is, however, difficult to implement, so generally it can be fulfilled only on the average. Although this inexact realization of the constraint can be meaningful in the study of the properties of real materials, it can also encode some unwanted features. For example, if the subject of the study is spin mediated superconductivity, it is not clear whether the analysis will be spoiled by the valence fluctuations of the f-impurity electrons or not. Moreover, as the Kondo lattice is an effective description of the Anderson lattice, it would be reasonable to be able to solve it without any reference to the high-energy physics that is integrated out by the Schrieffer-Wolff procedure. Only in this way can one expect to learn something about the low-energy physics of the system and the driving mechanisms and interactions that are relevant at this low-energy scale.

From this point of view, we believe that it could be fruitful to represent the Kondo lattice Hamiltonian in terms of properly defined fermionic degrees of freedom: a formulation of the problem that *requires no implementation of the constraint, but is given anyway in terms of fermions only*. In this paper, we elaborate and discuss such a representation, identifying the map between the old degrees of freedom (impurity spins and conduction electrons) to the new ones (three spinless fermions c, g, and f). For sake of clarity, we will refer to this transformation as the cgf map in the rest of this manuscript. It is important to remark on the fact that our approach holds only for the KLM with spin-$1/2$ impurities.

The mapping could simply be defined and proved by brute force calculation, but we will also show the path that we followed to discover it, believing that a more pedagogical approach will make our method more interesting. The derivation goes through the representation of the electron and spin operators in terms of their basic Majorana fermion constituents. Writing the Kondo lattice Hamiltonian in terms of Majorana fermions [40], we treat the electrons and the spins on equal footing, avoiding the most problematic feature of the Hamiltonian. Our cgf map is a practical example of the usefulness of this Majorana fermion based approach.

Although the map holds for any number of dimensions and any lattice structure, we will study only the one-dimensional case at zero temperature, in order to have a comparison with the existing literature. We will perform a mean-field, zero-temperature analysis of the KLM, represented on the set of the three spinless fermions. It will become clear how our treatment is able to naturally include, *already at the mean-field level*, all the three main mechanisms of RKKY interaction, local Kondo-singlet formation and double exchange. In particular, our approach very conveniently describes the latter two effects, permitting a mean-field analysis of the ferromagnetic regions of the phase diagram, on which we focus our attention.

Considering the length of this manuscript and the large amount of physics that we are going to discuss, we introduce here briefly the results of the mean-field analysis that we hope will convince the reader of the relevance of our work.

Our mean-field results are in good agreement with the picture recently provided by density matrix renormalization group (DMRG) [41] and dynamical mean-field theory (DMFT) [42] studies of the ferromagnetic metallic phase for low to intermediate values of the Kondo coupling. In fact, we identify a phase (FM-I) where we obtain a *quantitative agreement* on the values of the average on-site total magnetization and of the "commensurability parameter." For the latter, we provide also a theoretical justification, identifying the symmetry operation that enforces it. In the same phase, we recognize the fundamental role of the double-exchange mechanism, which allows for the generation of the "spin-selective Kondo insulator" (SSKI) and the separation of the electrons in majority and minority electrons. While the majority electrons behave as normal noninteracting electrons, the minority electrons appear only as constituents of delocalized Kondo singlets, as made explicit by the disappearance of their Fermi surface. The generation of the SSKI stabilizes the FM-I phase, but this does not mean that ferromagnetic order needs the realization of the SSKI. In fact, for low couplings, we discovered that the ferromagnetic phase can extend up to half-filling, but for a coupling-dependent critical density n^{F}_{crit}, the mechanism stabilizing the ferromagnetic order of the impurity spins changes completely, marking the emergence of a new phase FM-II. The transition from the FM-I and FM-II phases happens approximately at the known [35] phase-separation line that divides the ferromagnetic metallic and the paramagnetic phases. We believe that the FM-II phase is an improvement with respect to the RKKY-ferromagnetic state, able to incorporate the Kondo effect in a more efficient way. This property permits the FM-II phase to survive up to half-filling, if the coupling is not too strong. This phase is energetically competitive, if compared to the usual spiral ordered mean-field trial [37,38] ground states. In the light of these features, the FM-II state is a natural candidate for the description of the ferromagnetic "tongue" phase identified [35] inside the paramagnetic dome by DMRG simulations.

For intermediate couplings, an instability appears and the ferromagnetism of FM-II ceases to exist. In these situations, another coupling-dependent critical density $n^{\mathrm{pol}}_{\mathrm{crit}}$ appears for the FM-I phase. Above this density, we found no translational invariant mean-field solutions, except the half-filled one. In proximity of $n^{\mathrm{pol}}_{\mathrm{crit}}$, we note that the compressibility of the FM-I phase tends to infinity, so we interpret this feature as an indication of the fact that the two components forming the FM-I state (the majority electrons and Kondo-singlets liquids) start to separate. This process creates in the phase diagram a region of phase coexistence between the FM-I and the half-filled Kondo Insulating (KI) phase, where the latter is characterized by the absence of free electron modes. The location in the phase diagram and the physical picture of this region, in correspondence of the disappearance of the FM-II phase, are in good agreement with the description of the polaronic liquid provided by bosonization [2,3,29]. In terms of the qualitative two-liquid picture mentioned previously, the polarons can be identified as the "islands" of ferromagnetic FM-I phase immersed in the liquid of Kondo singlets of the half-filled KI phase.

Increasing even more the coupling the solutions become less and less meaningful. We believe that this is a symptom of the fact that the assumptions behind our mean-field approximation are not justified anymore.

Unfortunately, our mean-field decomposition scheme is not very convenient for the study of different kinds of magnetic orders, because the form of the Kondo Hamiltonian in terms of fermions c, g, and f is naturally suited for solutions that are translationally invariant. Consequently, we decided to not perform an analysis of the RKKY-liquid phase [1,35], believing that a different kind of approach would be more convenient [43]. Instead, we briefly discuss the half-filled case, though we refer to the literature for a more appropriate approach [40,43], still based on the Majorana representation of the Kondo lattice Hamiltonian. At half-filling, we found a translational invariant KI solution, composed by a coherent superposition of local Kondo singlets; this solution becomes an energetically favorable ground state, at high couplings, if compared with the usual Neél ordered one. These features are consistent with the known results [1,17–20]. This KI ground state tends for $J \to +\infty$ to the correct ground state, where on each site a Kondo singlet is formed; moreover, it disappears if a J-dependent critical chemical potential $\mu^{\rm pol}_{\rm crit}(J)$ is reached. This chemical potential is the energy necessary to remove an electron from the system, therefore it must correspond to the quasiparticle gap [1,32]. The evolution of $\mu^{\rm pol}_{\rm crit}(J)$ with the coupling agrees very well with the results obtained via perturbative approaches [1], at high coupling, but does not share the same behavior away from this limit.

Showing the wide range of physics that can be described by following our approach to the problem, made possible by the representation of the Hamiltonian in terms of Majoranas, we hope to convince the reader that it could be interesting and profitable to tackle some of the open problems in condensed matter physics using the same line of thought. Moreover, we hope to provide the community with a new convenient starting point for the study of the KLM and, in particular, the study of its ferromagnetic properties in one and many dimensions.

The paper is organized as follows. In Sec. II, we represent faithfully the Kondo lattice Hamiltonian in terms of Majorana fermions [40] and review the known [44,45] typical properties common to these kind of mappings. Starting from this different formulation of the Hamiltonian we build the set of three spinless fermions in Sec. III. After a discussion of the properties and the meaning of the different spinless fermions, we will proceed in Sec. IV to the mean-field analysis of the phase diagram, focusing on the one-dimensional case at zero temperature. At the end, we provide also a final outlook.

II. MAJORANA MAP

In a recent work [40], it has been proved how the Kondo lattice Hamiltonian

$$H_K = -t \sum_{\sigma} \sum_{\langle i,j \rangle} c^{\dagger}_{c,\sigma}(\mathbf{r}_i) c_{c,\sigma}(\mathbf{r}_j) + \text{H.c.} - \mu^* \sum_i n_c(\mathbf{r}_i) + J \sum_i \mathbf{S}_c(\mathbf{r}_i)\, \mathbf{S}_f(\mathbf{r}_i) \qquad (1)$$

can be rewritten in terms of six Majorana fermion degrees of freedom (Majoranas). In the previous equation, J is the Kondo coupling, S_c and S_f are, respectively, the electron- and impurity-spin operators, n_c is the conduction electron operator, μ^* is the Lagrange multiplier of the density constraint (i.e., the chemical potential), and $\langle i,j \rangle$ indicates the usual sum over nearest neighbors.

To understand the Majorana formulation, it is enlightening to start from the symmetric one-site (local) Anderson impurity model and analyze its Fock space. The Hamiltonian is given by

$$H_{1A} = -V \sum_{\sigma=\uparrow,\downarrow} (c^{\dagger}_{c,\sigma} c_{f,\sigma} + c^{\dagger}_{f,\sigma} c_{c,\sigma}) + U(n_f - 1)^2, \quad (2)$$

where the subscripts c, f denote two different fermion species (two different orbital indices) and U, V are real parameters. It is well known [7,15,36,39] that in the limit $U, V \to +\infty$, with $J = 4V^2/U$, the Hamiltonian (2) generates exactly the spin-spin interaction term in (1); hence the total Hilbert space of the local (one-site) Kondo lattice model can be interpreted as the low-energy eight-dimensional subspace of the original 16-dimensional local Anderson Fock space. The energy separation of the two subspaces is due to the interaction term $U(n_f - 1)^2$ that brings no corrections to the energy for $n_f = 1$, while it gives a contribution proportional to U in case $n_f = 0$ or 2. For $U \to +\infty$, the states with $n_f = 0,2$ become inaccessible, so the states that span the low-energy Hilbert space are those with one f electron per site. This also means that the f-electron charge oscillations in the system are infinitely suppressed. As a consequence, the Kondo lattice model can be thought of as an Anderson impurity lattice model where the f electron density obeys the *exact* local constraint $n_f = 1$.

The Majorana fermion description of the Kondo lattice model [40] stems from these considerations, but implements them in a completely different way. Starting from the one-site Anderson Hamiltonian, it is possible to set up a nonlinear canonical transformation [46] that separates the local Hilbert space in two sectors of low and high energy. The connection between the two spaces is given by a fermion operator $c^{\dagger}_4$, whose density is the only operator proportional to U in the Hamiltonian. The local Kondo Hilbert space is then given by the states that contain no c_4 fermion. It is thus possible to show [40] that the Hamiltonian (1) can be rewritten using Majorana fermion degrees of freedom (Majoranas). We define the Majoranas [47–49] in terms of our original operators in (1) via

$$c^{\dagger}_{c,\uparrow}(\mathbf{r}_i) = \frac{\gamma_1(\mathbf{r}_i) + i\gamma_2(\mathbf{r}_i)}{\sqrt{2}}, \qquad (3)$$

$$c^{\dagger}_{c,\downarrow}(\mathbf{r}_i) = \frac{-\gamma_3(\mathbf{r}_i) + i\gamma_4(\mathbf{r}_i)}{\sqrt{2}}, \qquad (4)$$

$$S^x_f(\mathbf{r}_i) = -i\mu_2(\mathbf{r}_i)\mu_3(\mathbf{r}_i), \quad S^y_f(\mathbf{r}_i) = -i\mu_3(\mathbf{r}_i)\mu_1(\mathbf{r}_i), \quad S^z_f(\mathbf{r}_i) = -i\mu_1(\mathbf{r}_i)\mu_2(\mathbf{r}_i), \qquad (5)$$

with the convention for the Clifford algebra of the Majorana operators: $\{\alpha_i, \beta_j\} = \delta_{i,j}\delta_{\alpha,\beta}$, that means $\alpha_i^2 = 1/2$, where $i, j = 1,2,3$ and α, β can be both γ and μ.

The faithful representation of the Kondo lattice Hamiltonian is obtained replacing the Majorana $\gamma_4(\mathbf{r}_i)$ with the γ-independent Majorana $\gamma_0(\mathbf{r}_i) = 2i\mu_1(\mathbf{r}_i)\mu_2(\mathbf{r}_i)\mu_3(\mathbf{r}_i)$, so that

$$c^{\dagger}_{c,\downarrow}(\mathbf{r}_i) = \{-\gamma_3(\mathbf{r}_i) + i\,[2i\mu_1(\mathbf{r}_i)\mu_2(\mathbf{r}_i)\mu_3(\mathbf{r}_i)]\}/\sqrt{2}.$$

In these terms, the Kondo Hamiltonian (1) is rewritten as

$$H_M = -it\sum_{n,\delta}[\gamma_2(\mathbf{r}_n)\gamma_1(\mathbf{r}_n+\boldsymbol{\delta}) - \gamma_1(\mathbf{r}_n)\gamma_2(\mathbf{r}_n+\boldsymbol{\delta}) + \gamma_3(\mathbf{r}_n)\gamma_0(\mathbf{r}_n+\boldsymbol{\delta}) - \gamma_0(\mathbf{r}_n)\gamma_3(\mathbf{r}_n+\boldsymbol{\delta})]$$
$$+\frac{J}{4}\sum_n\{i\gamma_1(\mathbf{r}_n)\mu_1(\mathbf{r}_n) + i\gamma_2(\mathbf{r}_n)\mu_2(\mathbf{r}_n) + i\gamma_3(\mathbf{r}_n)\mu_3(\mathbf{r}_n) + 2[\gamma_2(\mathbf{r}_n)\mu_2(\mathbf{r}_n)\gamma_3(\mathbf{r}_n)\mu_3(\mathbf{r}_n)$$
$$+\gamma_1(\mathbf{r}_n)\mu_1(\mathbf{r}_n)\gamma_3(\mathbf{r}_n)\mu_3(\mathbf{r}_n) + \gamma_1(\mathbf{r}_n)\mu_1(\mathbf{r}_n)\gamma_2(\mathbf{r}_n)\mu_2(\mathbf{r}_n)]\} - \mu^*\sum_n[-i\gamma_1(\mathbf{r}_n)\gamma_2(\mathbf{r}_n) - i\gamma_0(\mathbf{r}_n)\gamma_3(\mathbf{r}_n) + 1], \quad (6)$$

where $\mathbf{r}_n$ is summed over every lattice site and $\boldsymbol{\delta}$ are the Bravais lattice vectors; so, for example, in the one-dimensional case, $\sum_{n,\delta}\gamma_2(\mathbf{r}_n)\gamma_1(\mathbf{r}_n+\boldsymbol{\delta}) = \sum_n\gamma_2(\mathbf{r}_n)\gamma_1(\mathbf{r}_{n+1})$.

This reformulation of the Kondo lattice Hamiltonian, although derived from the Anderson picture (2), has the major advantage of being constraint free and of treating the degrees of freedom of both the electron and the localized spin on equal footing. To the best of our knowledge, there exists no other formulation of the Kondo lattice model that realizes these two features simultaneously.

The reader should keep in mind that the Majorana γ_0 is composed by the three Majoranas μ_1,μ_2,μ_3. In a recent work [43], we analyzed this dual nature of the Majorana γ_0, suggesting that this Majorana fermion should be the correct degree of freedom to describe the system for small values of the coupling J. However, in the present work, we take a different approach, and we will instead consider γ_0 as a short-hand notation to indicate the three-body object $2i\mu_1\mu_2\mu_3$.

The proof of Eq. (6) has been already outlined [40], but thanks to the identification of the cgf map we will be able to provide a more straightforward derivation of it in this manuscript.

The cgf map generates a new representation of the degrees of freedom of the system, in terms of fermions only. This is formally made possible by a *nonlinear transformation* of the original spin and fermionic operators, which is easily set up working in terms of Majorana fermions, rather than the original operators. The use of these kind of nonlinear transformations is not new to the literature; for example, it has been used in the study of the Hubbard model [44,45]. In that context, it has been shown how the fermionic operators representing the degrees of freedom of the conduction electrons can be expressed in terms of a fermionic operator (describing the holon) and three spin operators (describing the spinon). In order to fully understand this approach, it is appropriate to review and discuss some known properties of the fermionic operators and their representation in terms of Majoranas. This is done in Appendix A. We invite the reader who is not familiar with these topics and in particular with the holon-spinon representation to examine the appendix, in order to get more insight on the transformation realized by the cgf map that we are going to introduce in the next section.

III. THE CANONICAL CGF-MAP

In light of the previous paragraphs and the information contained in Appendix A, it becomes possible to give a better interpretation of the Majorana map that generates Eq. (6). The only Majoranas that appear in H_M are the three coming from the original conduction c electron $\gamma_1,\gamma_2,\gamma_3$ and the three coming from the frozen f electron μ_1,μ_2,μ_3 (to avoid cluttering of the notation, we suppress the local index $\mathbf{r}_n$ and we refer always to the local Hilbert space if not specified otherwise). The creation of the spinful c electron is given by the spinor operator

$$c_c^\dagger = \begin{pmatrix} c_{c,\uparrow}^\dagger \\ c_{c,\downarrow}^\dagger \end{pmatrix} = \begin{pmatrix} \frac{\gamma_1+i\gamma_2}{\sqrt{2}} \\ \frac{-\gamma_3+i(2i\mu_1\mu_2\mu_3)}{\sqrt{2}} \end{pmatrix}. \quad (7)$$

Therefore it is immediate to identify (up to a $-\pi/2$ irrelevant phase factor) the second component of the spinor operator (7) as the creation operator of the holon associated to a (hyper-)spinful particle described by the operator $s^\dagger$:

$$s^\dagger = \begin{pmatrix} \frac{\mu_1+i\mu_2}{\sqrt{2}} \\ \frac{-\mu_3+i\gamma_3}{\sqrt{2}} \end{pmatrix}. \quad (8)$$

It is then clear that it becomes possible to associate to each local quantum state of the Kondo lattice model the quantum numbers of a single fermionic particle characterized by a generalized spin, generated by an intrinsic symmetry group different from SU(2). From this point of view the involved structure given by (7) and (8) can be easily understood, characterized and generalized. Such classification is irrelevant for the present work, so we will leave this for future discussion [50].

Instead, we will take a much easier and straightforward direction in the following, considering the components of this higher-dimensional spinor as independent spinless particles, in the same fashion as the usual separation of the spinor (7) in components $c_{c,\uparrow}^\dagger$ and $c_{c,\downarrow}^\dagger$. In practice, we consider three spinless fermions: one for each independent component of the previous spinor, i.e., one for the first (up) component of (7) and two for (8).

We name these three spinless fermions after the definition of their creation/annihilation operators:

$$c^\dagger = \frac{\gamma_1+i\gamma_2}{\sqrt{2}}, \quad g^\dagger = \frac{\gamma_3+i\mu_3}{\sqrt{2}}, \quad f^\dagger = \frac{\mu_1+i\mu_2}{\sqrt{2}}. \quad (9)$$

For future convenience, with respect to (8), we have added an extra $-\pi/2$ phase factor in the definition of $g^\dagger$.

Having defined these operators, we need only to prove that the local Fock space on which they act is (isomorphic to) the local Hilbert space of the Kondo lattice model. This will also help us to understand the physical properties and meanings of these three particles. The creation operators (9) acting on their vacuum state $|0_{cgf}\rangle$ generate an eight-dimensional Fock space (note that the anticommutative relations between

TABLE I. States of the local Kondo Hilbert space expressed in terms of the original electron-spin quantum numbers (left) and the corresponding state in the cgf representation (right). The phase factors could be easily canceled, reabsorbing them into the definitions of the different operators, but these definitions are kept for future convenience and to maintain continuity in the notation of Appendix A and with the literature.

$-\|\Downarrow\rangle$	$\longleftrightarrow$	$g^\dagger\|0_{cgf}\rangle$
$-i\|\Uparrow\rangle$	$\longleftrightarrow$	$f^\dagger\|0_{cgf}\rangle$
$\|\downarrow\Downarrow\rangle$	$\longleftrightarrow$	$\|0_{cgf}\rangle$
$-\|\uparrow\Downarrow\rangle$	$\longleftrightarrow$	$c^\dagger g^\dagger\|0_{cgf}\rangle$
$i\|\downarrow\Uparrow\rangle$	$\longleftrightarrow$	$g^\dagger f^\dagger\|0_{cgf}\rangle$
$-i\|\uparrow\Uparrow\rangle$	$\longleftrightarrow$	$c^\dagger f^\dagger\|0_{cgf}\rangle$
$\|\uparrow\downarrow\Downarrow\rangle$	$\longleftrightarrow$	$c^\dagger\|0_{cgf}\rangle$
$i\|\uparrow\downarrow\Uparrow\rangle$	$\longleftrightarrow$	$c^\dagger g^\dagger f^\dagger\|0_{cgf}\rangle$

the operators is assured by the Clifford algebra structure of the Majorana operators), which has the same dimension as the local Hilbert space of the Kondo lattice model. As the three creation (annihilation) operators are expressible in terms of the original electron and impurity-spin operators, it is clear that if $|0_{cgf}\rangle$ belongs to the Kondo local Hilbert space, then the other states will also belong to it. A simple calculation shows that

$$c^\dagger = c^\dagger_{c,\uparrow}, \tag{10}$$

$$g^\dagger = -\tfrac{1}{2}\left[c^\dagger_{c,\downarrow} + c_{c,\downarrow} + (c^\dagger_{c,\downarrow} - c_{c,\downarrow})2S^z_f\right], \tag{11}$$

$$f^\dagger = -i(c_{c,\downarrow} - c^\dagger_{c,\downarrow})S^+_f. \tag{12}$$

We remind the reader that in our model $S^2_f = 3/4$.

Looking in the local Kondo Hilbert space for the state $|0_{cgf}\rangle$, such that $c|0_{cgf}\rangle = g|0_{cgf}\rangle = f|0_{cgf}\rangle = 0$, it is easy to show that

$$|0_{cgf}\rangle = (c^\dagger_{c,\downarrow}|0\rangle_c) \otimes |\Downarrow\rangle_f = |\downarrow\Downarrow\rangle, \tag{13}$$

where $|0\rangle_c$ is the vacuum of the original conduction electrons $c_{c,\downarrow}|0\rangle_c = c_{c,\uparrow}|0\rangle_c = 0$, and $|\Downarrow\rangle_f$ is the spin-down state of the original impurity spin $S^-_f|\Downarrow\rangle_f = 0$. The relations between the other states follow naturally. We report the complete structure of the map in Table I, that together with the formulas (10)–(12) represents the core of our work, the cgf map.

Clearly, in principle, it is not necessary to take the Majorana approach to generate the cgf map. However, it seems improbable that a different path for the derivation could be followed, considering the complicated structure of the fermionic operators generated. The power of the analysis in terms of Majoranas stems from the relative easiness of the generation of involved transformations that mix both fermion and spin operators.

Now that the spinless fermions c, g, and f have been introduced, it is possible to represent the Hamiltonian (1) making use of the cgf map. A direct calculation, that is, very much simplified, starting from (6), leads to

$$H_{cgf} = H_c + H_{de} + H_J + H_{\rm chem}. \tag{14}$$

In which

$$H_c = -t\sum_{n,\delta}(c^\dagger\tilde{c} + \tilde{c}^\dagger c), \tag{15}$$

$$H_{de} = +t\sum_{n,\delta}\left(\frac{1}{2} - f^\dagger f\right)(g^\dagger - g)(\tilde{g}^\dagger + \tilde{g}) - \left(\frac{1}{2} - \tilde{f}^\dagger\tilde{f}\right)(g^\dagger + g)(\tilde{g}^\dagger - \tilde{g}), \tag{16}$$

$$H_J = \frac{J}{4}\sum_n(1 - c^\dagger c - f^\dagger f - g^\dagger g + 2c^\dagger c f^\dagger f) + \frac{J}{4}\sum_n 2g^\dagger g[i(c^\dagger f - f^\dagger c)]. \tag{17}$$

The last term $H_{\rm chem}$ is given by the chemical potential term:

$$H_{\rm chem} = -\mu^*\sum_n(c^\dagger c - f^\dagger f - g^\dagger g + 2f^\dagger f g^\dagger g + 1).$$

In all the previous equations, we have used the same conventions of (6) with the prescription that a generic operator α without the tilde stands for $\alpha(\mathbf{r}_n)$, while $\tilde{\alpha}$ represents $\alpha(\mathbf{r}_n + \boldsymbol{\delta})$. The term H_{de}, which is the most unusual one in the Hamiltonian (14), describes a density-correlated hopping for the g fermions and is responsible for the description of the double-exchange mechanism. It is the appearance of this term that makes this three-fermion representation of the Kondo lattice very successful in the description of ferromagnetism, as will be made clear by the mean-field analysis in the next section. We stress that these kinds of nontrivial hopping structures are a typical consequence of the nonlinear transformations of the type (7). Similar situations are encountered, for example, in both the context of the one-band Hubbard model [44,45] and the t-J model [51].

It is evident that Hamiltonian (14), the mapping of Table I and the equations (10)–(12), can be demonstrated by *direct inspection*, without passing through the procedure that produces H_M. In fact, one can simply consider Hamiltonian (14), i.e., the cgf form of (6), as an ansatz, and then using formulas (10)–(12) the usual Hamiltonian (1) of the KLM is recovered. Hence, using the very general definitions of (9), the cgf map generates a different, indirect and alternative demonstration of the faithful Majorana representation of the Kondo lattice model given by (6) and (7).

To understand the meaning of the three fermions (9), it is useful to express some physically interpretable operators in terms of them. The easiest expressions are given for the spin-up conduction electron density and the impurity $\hat{z}$-oriented spin operator:

$$c^\dagger_{c,\uparrow}c_{c,\uparrow} = c^\dagger c, \quad S^z_f = f^\dagger f - \tfrac{1}{2}. \tag{18}$$

Of much greater interest is the density operator of the spin-down component of the conduction electron:

$$c^\dagger_{c,\downarrow}c_{c,\downarrow} = 1 - f^\dagger f - g^\dagger g + 2f^\dagger f g^\dagger g. \tag{19}$$

This operator, quadratic in the original representation, becomes partly quartic if represented on the cgf operators. This is not surprising, considering that the map is built on the idea

that the $c_{c,\downarrow}$ electron must be interpreted as the holon of (8). Given that two particles contribute to the constitution of the $c_{c,\downarrow}$ fermion, it must happen that their densities sum up properly. In a more concrete fashion, it is possible to think that the electric charge density associated with the fermion degree of freedom $c_{c,\downarrow}$ (i.e., the down component of the physical electron mode of charge $e = 1$), decomposes into two channels given by the two primitive particles of which it consists. The nonquadratic form of the chemical potential term H_{chem} is a direct consequence of (19). The coefficient μ^* will determine not only the amount of total electric charge density (as it does in the usual linear case), but it will affect also how the density of $c_{c,\downarrow}$ electrons is redistributed between the two channels g and f.

Although unconventional, this technique of fermion decomposition is not a complete novelty in the literature. Similar approaches have been followed, for example, in the study of the t-J model [51] and in a quite general fashion we can classify them into the framework of generalized Bogoliubov transformations.

Substituting (18) into (19), we can rewrite

$$c^\dagger_{c,\downarrow} c_{c,\downarrow} = \tfrac{1}{2} + \left(g^\dagger g - \tfrac{1}{2}\right) 2S^z_f \tag{20}$$

or

$$g^\dagger g = \left(c^\dagger_{c,\downarrow} c_{c,\downarrow} - \tfrac{1}{2}\right) 2S^z_f + \tfrac{1}{2}. \tag{21}$$

The latter equation displays the nature of the g-fermion density: it is generated by the original $c_{c,\downarrow}$ density and an impurity-spin–dependent particle-hole transformation $c_{c,\downarrow} \leftrightarrow c^\dagger_{c,\downarrow}$. Schematically, we have on each generic local state $|\alpha\rangle$,

$$\text{if} \quad S^z_f|\alpha\rangle = \tfrac{1}{2}|\alpha\rangle, \text{ then } c^\dagger_{c,\downarrow} c_{c,\downarrow} = g^\dagger g, \tag{22}$$

$$\text{if} \quad S^z_f|\alpha\rangle = -\tfrac{1}{2}|\alpha\rangle, \text{ then } c^\dagger_{c,\downarrow} c_{c,\downarrow} = 1 - g^\dagger g. \tag{23}$$

This means that the density operator $g^\dagger g$ counts the number of down-spin conduction electrons (holes) on the sites where the local impurity points up (down).

It is evident that the g and f fermions represent very nontrivial spin-electron excitations, whose nature will be made understandable by our mean-field analysis. However, in this section, it is appropriate to point out an intriguing parallelism between our f fermion and the composite fermion used in the large-N approximation. In large-N studies of the Kondo lattice, an auxiliary fermion operator is used to represent the local spins [14,15]. Because of the Kondo interaction, this auxiliary fermion develops dynamics and becomes the most intriguing excitation of the system: the heavy fermion. This heavy fermion is shown to have a composite nature: it is a bound state of the local spin and the conduction electron. In particular, it binds the creation of a conduction electron to a spin-flip of the impurity-spin on the same site. It is evident from (12) that our f fermion is very similar to this large-N composite fermion. There are, of course, some differences (in particular, the particle-hole linear combination of the conduction electrons), but this parallelism of our formalism with the more known and quite successful large-N approximation is very interesting.

IV. MEAN-FIELD ANALYSIS

As a first approach to the Hamiltonian (14), we perform a mean-field study to explore the possible ground states and understand the nature of the degrees of freedom that we are using to describe the system. To follow this path, the symmetries of H_{cgf} must be identified. The analysis of the symmetries can be easily done also if the Hamiltonian is written down in the Majorana representation (6), looking for the operators that commute with it. Among them we identify the nontrivial operator

$$\begin{aligned} A_3(n) &= -i\gamma_1(n)\gamma_2(n) - i\mu_1(n)\mu_2(n) \\ &= c^\dagger(n)c(n) + f^\dagger(n)f(n) - 1. \end{aligned} \tag{24}$$

It is straightforward to check that [52]

$$\left[H, \sum_n A_3(n)\right] = 0. \tag{25}$$

In the previous two equations we used the index n instead of $\mathbf{r}_n$ as site index. In our mean-field analysis, we decided to enforce the symmetry (25), so we imposed the commutation between the mean-field cgf-Hamiltonian H^{MF}_{cgf} and the operator $\sum_n A_3(n)$. The rationale behind this choice is that the breaking of this symmetry is a necessary condition for superconductivity that we do not wish to include in the study. In fact, the consequences of our choice are

$$\begin{aligned} &\langle c^\dagger f^\dagger\rangle = \langle g^\dagger c^\dagger\rangle = \langle g^\dagger f^\dagger\rangle = 0, \\ &\langle g^\dagger f\rangle = \langle g^\dagger c\rangle = 0, \\ &\langle f^\dagger \tilde{g}^\dagger\rangle = \langle f^\dagger \tilde{g}\rangle = \langle \tilde{f}^\dagger g^\dagger\rangle = \langle \tilde{f}^\dagger g\rangle = 0. \end{aligned} \tag{26}$$

This means that there exist no open channel for the hybridization of the g fermions with c and f fermions, so the pairing order parameter $\langle c_{c,\uparrow} c_{c,\downarrow}\rangle$ will always be zero, as can be checked using the formula

$$c_{c,\downarrow} = -g^\dagger - f^\dagger f(g - g^\dagger),$$

and making use of Wick's theorem to decompose the higher-order operators.

The enforcement of this symmetry hides some very subtle and unexpected surprises. In fact, rewriting (24) in terms of the usual impurity-spin and conduction-electron operators, we obtain

$$\begin{aligned} A_3 &= \tfrac{1}{2}\big\{2S^z_f + (c^\dagger_{c,\uparrow} c_{c,\uparrow} + c^\dagger_{c,\downarrow} c_{c,\downarrow}) \\ &\quad + (c^\dagger_{c,\uparrow} c_{c,\uparrow} - c^\dagger_{c,\downarrow} c_{c,\downarrow}) - 1\big\} \\ &= \tfrac{1}{2}\big(2S^z_f + n_c + 2m - 1\big), \end{aligned} \tag{27}$$

where the site index n has been suppressed to not clutter the notation. This implies the existence of a very nontrivial relation between the electron magnetization $\langle m\rangle = \langle c^\dagger_{c,\uparrow} c_{c,\uparrow} - c^\dagger_{c,\downarrow} c_{c,\downarrow}\rangle/2$, the electron density $\langle n_c\rangle = \langle c^\dagger_{c,\uparrow} c_{c,\uparrow} + c^\dagger_{c,\downarrow} c_{c,\downarrow}\rangle$, and the spin polarization $\langle S^z_f\rangle$. The existence of this nontrivial relation has been recently discovered numerically making use of DMFT + NRG methods [42] (NRG stands for "numerical renormalization group") in infinite dimensions and DMRG [41] in the one-dimensional case. To be consistent with the literature, we call the A_3 operator the "commensurability operator." The sign differences between our definition of

commensurability and the one that can be found in the numerical studies [41,42] is due to an opposite convention for the up direction of the spin polarization axis.

Therefore the first concrete result of our analysis is the identification of this symmetry, which furnishes a theoretical justification to the "commensurability" parameter. We want to remark that we have not yet restricted our analysis to the one-dimensional case, but we are still dealing with an arbitrary number of dimensions, therefore these conclusions refer to both the DMRG [41] and the DMFT + NRG results [42].

It is useful for the discussion to write down explicitly the form of $H^{\rm MF}_{cgf}$ obtained enforcing the symmetry (25):

$$H^{\rm MF}_{cgf} = H^{\rm MF}_{cf} + H^{\rm MF}_{g} + H^{\rm MF}_{\rm chem} + H^{\rm MF}_{\rm shift}, \tag{28}$$

where

$$H^{\rm MF}_{cf} = -t\sum_{n,\delta}(c^\dagger \tilde{c} + \tilde{c}^\dagger c) + t\sum_{n,\delta}\left(\frac{1}{2} - f^\dagger f\right)\mathcal{S}_n - \left(\frac{1}{2} - \tilde{f}^\dagger \tilde{f}\right)\mathcal{P}_n$$
$$+ \frac{J}{4}\sum_n 2\,(\mathcal{G}_n + \mathcal{I}_n)\,[i(c^\dagger f - f^\dagger c)] - 2\mathcal{R}_n(c^\dagger f + f^\dagger c) + \sum_n (2\mathcal{C}_n - 1) f^\dagger f + (2\mathcal{F}_n - 1)c^\dagger c, \tag{29}$$

$$H^{\rm MF}_{g} = t\sum_{n,\delta}\left(\frac{1}{2} - \mathcal{F}_n\right)(g^\dagger - g)(\tilde{g}^\dagger + \tilde{g}) - \left(\frac{1}{2} - \mathcal{F}_{n+1}\right)(g^\dagger + g)(\tilde{g}^\dagger - \tilde{g}) + \frac{J}{4}\sum_n (-1 - 4\mathcal{I}_n) g^\dagger g, \tag{30}$$

$$H^{\rm MF}_{\rm chem} = -\mu^* \sum_n (c^\dagger c - f^\dagger f + 2\mathcal{G}_n f^\dagger f + 2\mathcal{F}_n g^\dagger g + 1), \tag{31}$$

and $H^{\rm MF}_{\rm shift}$ represents the total, mean-field dependent shift of the energy. The definitions for the various mean-fields are

$$\begin{aligned} &S_n = \langle (g^\dagger - g)(\tilde{g}^\dagger + \tilde{g})\rangle, \quad P_n = \langle (g^\dagger + g)(\tilde{g}^\dagger - \tilde{g})\rangle, \\ &\mathcal{I}_n = -\frac{i}{2}(\langle c^\dagger f\rangle - \langle f^\dagger c\rangle), \quad \mathcal{R}_n = \frac{1}{2}(\langle c^\dagger f\rangle + \langle f^\dagger c\rangle), \\ &\mathcal{F}_n = \langle f^\dagger f\rangle, \quad \mathcal{C}_n = \langle c^\dagger c\rangle, \quad \mathcal{G}_n = \langle g^\dagger g\rangle. \end{aligned} \tag{32}$$

With the subscript n we want to remark the fact that modulation of the mean-fields are allowed in general. Of course, modulations with wave vectors different from $\mathbf{K} = 0$ imply the study of larger unit cells.

The $H^{\rm MF}_{cf}$ describes a delocalized spinless fermion (electron) that hybridizes with a lattice of f impurities; while the $H^{\rm MF}_{g}$ is the fermionic representation of the generalized transverse field Ising model [53,54]. The exact dynamics of the two subsystems depend on the specific structure of the mean fields.

If $J = 0$, the c-f hybridization does not take place, so the f fermions give rise to a flat band, while the c fermions produce the usual multidimensional cosine-free band. When J is increased, the two species hybridize, causing the opening of a gap in the band structure, with the typical *avoided crossings*.

Although the $H^{\rm MF}_{g}$ has an unconventional form, it is important to stress that according to (18), one obtains

$$\mathcal{F}_n = \langle f^\dagger(n) f(n)\rangle = 1/2 - \left\langle S^z_f(n)\right\rangle, \tag{33}$$

therefore if the impurity-spin order parameter is constant in space (ferromagnetic order), then the g fermions are described by a simple noninteracting model, while any space modulation introduces p-wave pairing terms in the g Hamiltonian.

From these considerations, it is evident that the structure of the $\mathcal{F}_n$ field plays a central role in the mean-field Hamiltonian. In fact, it is the scattering of the g electrons on the modulations of $\mathcal{F}_n$ that causes the opening of a gap in the g band. Moreover, one should keep in mind that the magnitude of $\mathcal{F}_n$ also determines the bandwidth of the g-fermion band. This band renormalization is the most unconventional feature of the Hamiltonian (28) and it is remarkable, especially considering that we obtain it in a mean-field framework. Indeed, band renormalization effects do not typically appear in mean-field contexts, while they are obtained in more involved approximation schemes, such as Gutzwiller projection methods.

From all these considerations, it is clear that it is very difficult to predict the properties of the mean-field ground state, so that the only way to tackle the problem is numerically. We did it following the algorithm presented in Appendix B, generating a system of nonlinear equations whose solutions coincide with the values of the order parameters for the mean-field solutions. In order to find all the possible solutions of the nonlinear system, we created a grid in the entire parameter space and used each point of the grid as starting point for a Newton-Raphson root finder. We repeated this procedure for different values of chemical potential and Kondo coupling, mapping the full phase diagram [55]. This procedure permitted us to find not only the mean-field ground state, but also higher-energy mean-field states and to follow them in their complicated evolution in the phase diagram.

In the following, we will focus our attention on translationally invariant solutions, which should be dominant away from half-filling and from the weak coupling limit; therefore we will consider constant values for all the mean fields on the entire lattice. We must stress the fact that this does not mean that we are forcing the system into a ferromagnetic state. In fact, paramagnetic states, which posses this kind of translational invariant property, will still be, in principle, included into the sector of the theory that we are going to analyze. What will be excluded are states and effects that are characterized by nonlocal correlations between different sites. So we expect our solution to not be able to capture the physics of the RKKY liquid phase, for example. To describe (at the mean-field level) states that posses these kind of nonlocal correlations, we should allow for the spatial modulation of the mean fields. Only at the end, we will discuss this option, considering the

possibility of adding a staggered modulation for the mean fields, restricting the analysis to the half-filled system. In this way, it would be possible to see how the RKKY effect enters into the Hamiltonian and why antiferromagnetic or spiral orders can appear at mean-field level. Unfortunately, the analysis will reveal that a neat separation between the RKKY and Kondo effect is, in general, impossible. To go beyond the known results [38], we should allow for the competition of these two effects, but this would make the mean-field analysis more involved. Therefore, in this work, we do not consider this extremely general case that in our opinion should instead be tackled with different approximation schemes [43]. However, we will point out the connection with the known mean-field treatments of the RKKY effect in the KLM and provide a discussion of the half-filled system showing how the paramagnetic Kondo insulating phase becomes the mean filed ground state at high coupling. Since this phase is also translationally invariant, our mean-field study becomes quite meaningful and, in particular, very efficient in the analysis of the quasiparticle gap. Although our mean-field algorithm works for any temperature T and number of dimensions, we performed a study only in one dimension and in the $T \to 0$ limit; we leave the other cases for future studies.

A. Ferromagnetic solutions away from half-filling

We will now focus our attention on the results that we obtained imposing translational invariance, i.e., assuming a constant value of all mean fields on the entire lattice. The translational invariant Hamiltonian, which we indicate as H_{cgf}^{MFTI}, looks like

$$H_{cgf}^{\mathrm{MFTI}} = -t\sum_n c^\dagger \tilde{c} + \tilde{c}^\dagger c - 4t(\mathcal{S}-\mathcal{P})\sum_n f^\dagger f + \frac{J}{4}\sum_n 2(\mathcal{G}+\mathcal{I})[i(c^\dagger f - f^\dagger c)] + (2\mathcal{C}-1) f^\dagger f + (2\mathcal{F}-1)c^\dagger c$$
$$+ 2t\left(\frac{1}{2}-\mathcal{F}\right)\sum_n g^\dagger \tilde{g} + \tilde{g}^\dagger g + \frac{J}{4}\sum_n (-1-4\mathcal{I}) g^\dagger g + H_{\mathrm{chem}}^{\mathrm{MF}} + H_{\mathrm{shift}}^{\mathrm{MF}}, \tag{34}$$

where we put $\mathcal{R}=0$, without loosing generality and en passant we note that $\mathcal{S}-\mathcal{P} = \langle g^\dagger \tilde{g} + \tilde{g}^\dagger g\rangle$.

The g-fermion subsystem is described by a trivial noninteracting Hamiltonian. Therefore all the mean-fields $\mathcal{G}$ and $\mathcal{S}-\mathcal{P}$ may be computed analytically as functions of the other variables.

We analyzed the system for discrete values of the adimensional coupling parameter $x = J/t$ between 0.05 and 6 and for different values of the chemical potential, in order to have a description of the most relevant region of the (x-n_c) phase diagram. For each value of x and μ, the nonlinear system was solved and the free energy $E - TS - \mu^* N$ was used to order the different solutions and to identify the mean-field candidate ground state. In general, the final picture that we obtain can be split in four regions: the first at half-filling and the other three away from half-filling, respectively, at low coupling ($x \lesssim 2$), intermediate coupling ($2 \lesssim x \lesssim 3$), and high coupling ($x > 3$). In the second region, it is possible to obtain, from our mean-field analysis, quantitative information about the structure of the ground state for any value of the filling. Instead, in the last two regions, our approach becomes less efficient, providing only indications on the nature of the system.

In the low-coupling regime, we discovered the existence of two ferromagnetic phases FM-I and FM-II, divided by a second-order phase transition that takes place at the critical conduction electron density $n_{\mathrm{crit}}^F(J)$. This part of the phase diagram is plotted in Fig. 1, where it is possible to see how closely our line of phase boundary is, when compared with the one found by DMRG methods [35,41]. This result improves significantly the available previous [38] mean-field ones. In particular, we do not identify the unphysical (global Kondo-singlet-like) paramagnetic solution, discovered by other mean-field methods, but we correctly find a ferromagnetic state stabilized by the Kondo effect. This is remarkable, since we do not force the system to a magnetic sector, but just to a translationally invariant one. The paramagnetic solution appears only at half-filling, which is the only region of the phase diagram where such a solution is expected.

We invite the reader to not confuse the paramagnetism induced by nonlocal correlations, with the one that we analyze. The nonlocal kind of paramagnetism has been excluded by our study when we chose to not spatially modulate our mean

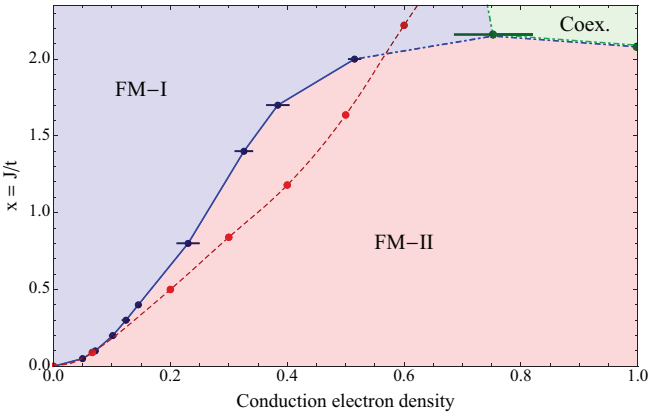

FIG. 1. (Color online) The $x = J/t$ vs n_c phase diagram. The thick continuous blue line represents the phase transition line between the FM-I and FM-II phases and should be compared with the dashed red line that shows the ferromagnetic-paramagnetic transition characterized by the DMRG calculations in Refs. [35] and [41]. The dashed blue line and the dot dashed green line represent the transition line between the ferromagnetic phases and the region of phase coexistence between the KI and the FM-I phases. The point at $x = 0$ is an extrapolation of the results, because our approach cannot be applied for that specific coupling value.

fields. In fact, the zone occupied by the paramagnetic states away from half-filling is instead covered by the FM-II state, which is a different kind of ferromagnetic phase.

It is important to point out how the FM-II phase at low coupling is a very competitive state, which has a better energy than the typical trial variational ground states [38] obtained via the introduction of spiral order in the impurity spins. This behavior marks the important role, also at low coupling, of the Kondo effect, which is able to stabilize a low-energy ferromagnetic state, if properly considered. Since it is well proved [2,3,56] that in this regime the spin-spin correlation function is peaked at $2k_F$, it is expected that variational states with (properly modulated) spiral spin order are energetically more competitive; the existence of the FM-II phase shows that the ordering of the spins alone is not enough to obtain a physically relevant trial ground state and the Kondo effect cannot be disregarded. Of course, these considerations are valid in the coupling regime that we considered. We did not perform any analysis of the extremely low-coupling regime, where it is not excluded that the spiral ordered states can become dominant.

1. *Ferromagnetism in the low-coupling limit*

In the coupling regime $x \lesssim 2$, we found for each value of μ^* and x two possible solutions. Varying the two parameters, these two solutions formed two sets of adiabatically connected mean-field states. One of the families was clearly very well separated in energy and so we discarded it, focusing only on the lowest (free) energy mean-field states. On this branch, as mentioned previously, it is possible to identify two different phases: the phase FM-I that extends from $n_c = 0$ to $n^F_{\rm crit}(J)$ and the phase FM-II that goes from $n_c = n^F_{\rm crit}(J)$ to 1. Though both the phases are ferromagnetic, they are characterized by different physical properties. In Fig. 2, we plot the values of the commensurability, total magnetization, and free energy versus the conduction electron density, using as example the coupling $x = 1.4$. Evidently, there exist a discontinuity in the behavior of these quantities at $n^F_{\rm crit} \approx 0.35$ that corresponds to the critical chemical potential $\mu_{\rm crit}/J \approx -1.1$. Such discontinuities in the derivatives of the curves continue to exist also if they are plotted with respect to the chemical potential, with the exception of the free energy. Indeed, as shown in Fig. 3, the free energy curve looks continuous and we were not able to resolve any discontinuity in the derivate. A more detailed analysis reveals the origin of the discontinuity in the derivate of the free energy curve in Fig. 2. Starting from the plots of the mean-field bands for the two phases FM-I and FM-II (some examples are plotted in Fig. 4), it is easy to understand how the system goes from the FM-I phase to the FM-II phase, via a Lifshitz transition[57], when the c-like band (curve always on the top in Fig. 4) crosses the Fermi level at zero energy. The discontinuity in the free energy versus the electron density is therefore due to the divergent contribution to the density of states, generated by the bottom of the c-like band that gets occupied. This is also consistent with the behavior of the density versus the chemical potential, where a vertical flex in correspondence of $n^F_{\rm crit}$ is present.

Focusing now on the FM-I phase, we identify this state with the ferromagnetic ground state discovered by DMRG

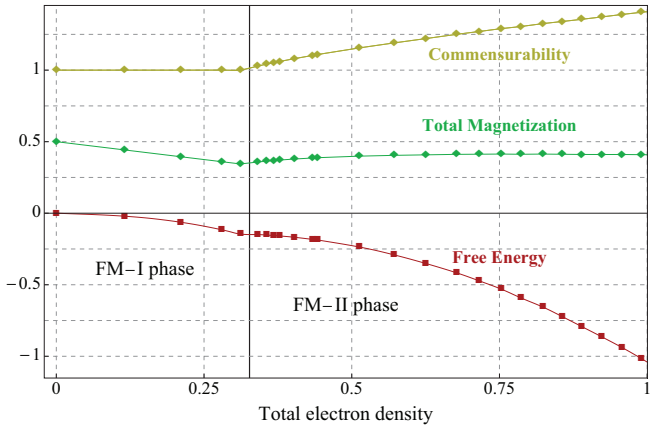

FIG. 2. (Color online) Free energy (plotted in units of $4t/\pi$) (red), total magnetization $\langle S_f \rangle + \langle c^\dagger_\uparrow c_\uparrow - c^\dagger_\downarrow c_\downarrow \rangle/2$ (green), and commensurability $\langle A_3 \rangle + 1 = \langle c^\dagger c + f^\dagger f \rangle$ (yellow) vs total electron density per site n_c, for the coupling $x = 1.4$. Evidently, in the FM-I phase, the magnetization is described by the known relation $|1 - \langle \hat{n}_c \rangle|/2$. The critical line (continuous vertical) is put in correspondence of the critical density $n^F_{\rm crit} \approx 0.35$. Beyond that value, the commensurability increases and the total magnetization becomes quickly almost constant. It is evident that there exists a discontinuity in the derivative of the free energy with respect to the electron density, which may indicate a phase transition of the Lifshitz kind, as explained in the text.

calculations. In fact, as shown, for example, in Fig. 2, we recognize that this state has a density-dependent total magnetization that correctly [1,41] goes linearly with the total electron density as $|1 - \langle n_c \rangle|/2$, starting from a totally ferromagnetic state at infinitesimal density [1,26]. It is also evident from Fig. 2 (but, of course, this is true for any ground state of the FM-I phase) that on the FM-I ground state the commensurability parameter is equal to one for each value of the electron density, exactly as in the DMRG solutions [41].

Beside these quantitative agreements, we discover that also the physical picture of the "spin-selective Kondo insulator" (SSKI) is perfectly consistent with the picture offered by our

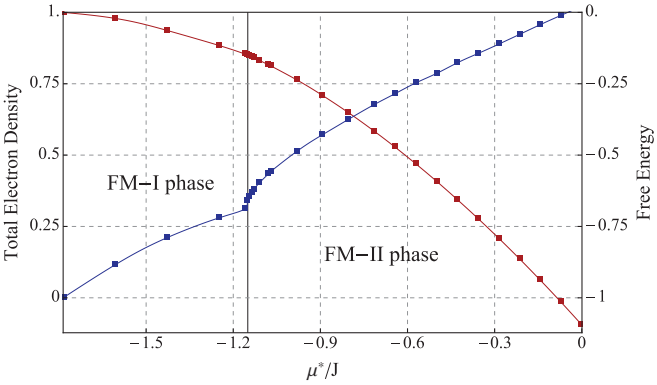

FIG. 3. (Color online) The free energy (plotted in units of $4t/\pi$) (red) and the total electron density (blue) vs the (rescaled) chemical potential μ^*/J for $x = 1.4$. The vertical flex of the density line, due to the contribution of the divergent density of state of the c-like band is very well visible.

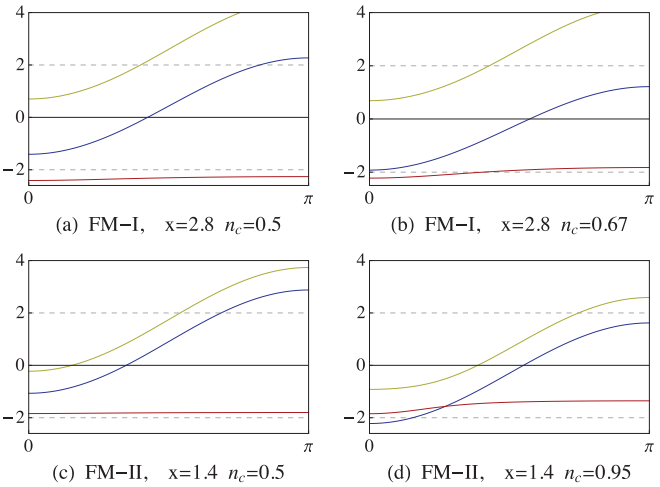

FIG. 4. (Color online) The cgf mean-field band structure for different parameter values. In (a) and (b), the FM-I band structure respectively at $x = 2.8$, $n_c \approx 0.5$ (i.e., $\mu^*/J = 1.8$) and $x = 2.8$, $n_c \approx 0.67$ (i.e., $\mu^*/J = 1.49$). In (c) and (d), the FM-II phase at $x = 1.4$, $n_c \approx 0.5$ (i.e., $\mu^*/J = 1.375$), and $x = 1.4$, $n_c \approx 0.95$ (i.e., $\mu^*/J = 0.2$). The g band (blue) presents always a Fermi surface at zero energy; in the FM-I phase, the yellow (c-like) band is completely empty, while in the FM-II phase it is partially filled. The red f-like band is instead always filled. The hybridization gap is well visible in all the plots. The band structure is symmetric under $k \to -k$ and on the y axis the energy is always given in units of t.

mean-field ground state in the FM-I phase. The physics behind the SSKI, as proposed in Refs. [41,42], is very interesting and our cgf description of the system exposes it perfectly. Starting from the one-conduction-electron limit, it is possible to understand the main features of this mechanism. The one-electron system is notoriously ferromagnetic as can be proved analytically [1,26] or understood invoking the double-exchange mechanism [2]. Indeed, since the electron hopping operator preserves the spin of the electron and considering that the system wants to maximize the energy gain from the antiferromagnetic coupling, it must happen that all the impurity spins align in the direction opposite to the spin of the only conduction electron present. This effect is taken into account in H_{cgf}^{MFTI} by the density-correlated g-hopping term (16): it is clear that in order to maximize the gain from the kinetic energy contribution, the system will develop ferromagnetism. Therefore, with an infinitesimal electron density, the result must be $\mathcal{F} = 1$, so that via (18) $\langle S_f^z \rangle = 1/2$ and the bandwidth of the g band is maximized [58]. It is easy to understand this process in the semiclassical picture, i.e., turning off the spin-flip part of the electron-impurity spins interaction and considering only the Ising-like part.

Inserting now more electrons into the system and considering the effect of the spin-flip processes that the electrons experience scattering against the impurity spins, the situation becomes more involved. The configuration where all the electrons share the same spin is not energetically optimal nor consistent with the existence of the electron-spin scattering, so also the band of $c_{c,\uparrow}$ electrons (minority-electrons) must be partially filled. This is problematic for the system, because the up electrons have spins parallel with the ferromagnetically ordered impurity spins (majority spins). To solve this problem, the system binds the minority-spins (generated by the scattering of the electrons against the ferromagnetically ordered majority spins) to the minority electrons, performing a sort of "effective annihilation," via the creation of Kondo singlets. The latter become the relevant objects of the system and the minority spins and minority electrons cease to exist as independent degrees of freedom, becoming only highly correlated components of the singlets. Of course, this process has to happen not just locally, but taking into account the delocalization of the singlets on the entire system. Obviously, the wave function of the quantum liquid formed by the delocalized Kondo singlets must be entangled with the one describing the Fermi liquid of the majority electrons, because also (part) of the $c_{c,\downarrow}$ must participate in the creation of the singlets.

These singlets are responsible for the formation [41,42] of the SSKI that is described by the two c-f hybridized bands (in the following called c-like and f-like bands) in the Figs. 4(a) and 4(b), where we chose to plot the mean-field band structure for the ground-state solution at $x = 2.8$, $n_c \approx 0.5$ and 0.67. The high value of the coupling has been chosen to give a better visualization of the features of the FM-I phase; anyway, all the ground states in this phase share the same characteristics. Of course at mean-field level, considering our assumptions (26), the entanglement of the two many-body wave functions is lost, so the partially filled g band represents (effectively) the band formed by the majority electrons that are not bound into the Kondo singlets.

The previous description gives a qualitative rationale for the unit value of the commensurability. The idea is that there must occur a fine-tuning between the density of the minority electrons and of the minority spins. Indeed, the creation of minority spins is energetically expensive; for any majority spin turned into a minority spin, there is a loss in the kinetic energy of the g fermions, because of the reduction of the mean-field $\mathcal{F}$. Therefore the density of the minority spins will be as small as possible, i.e., there will be an equal number of minority spins and minority electrons.

It is now clear that in our description, while the c fermions represent the minority-electrons, the f fermions represent the majority spins; thus the vacancies in the completely filled f band must represent the minority spins and hybridize with the c fermions. Imposing the same value for the densities of the minority electrons and minority spins, remembering that the average number of minority electrons is $\mathcal{C}$ and that the average number of minority spins is $1 - \mathcal{F}$, it is straightforward to obtain

$$\mathcal{C} = 1 - \mathcal{F} \quad \Rightarrow \quad \mathcal{C} + \mathcal{F} = 1.$$

This is exactly the justification provided in Ref. [41] for the unitary value of the commensurability parameter, given in terms of cgf fermions. As is evident, our cgf formalism fits perfectly the physics of the SSKI and therefore the FM-I phase.

We plot an enlightening outcome of our cgf map mean-field analysis in Fig. 5. The curves represent the momentum distribution of the conduction electron density operators. As can be seen, the Fermi surface of the $c_{c,\uparrow}$ minority electrons is completely destroyed by the hybridization and as a matter of fact the minority electrons are not expected to show any

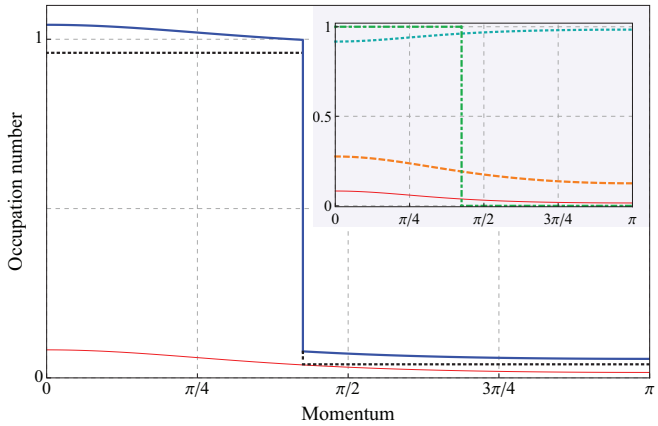

FIG. 5. (Color online) Expectation values on the FM-I cgf mean-field ground state at $x = 2.8$ and $n_c \approx 0.5$, corresponding to the band structure in Fig. 4(a). Momentum distribution on the Brillouin zone of the operators $n_{c,\uparrow}(k) = \langle c^\dagger_{c,\uparrow(k)} c_{c,\uparrow(k)} \rangle$ (thin red), $n_{c,\downarrow}(k) = \langle c^\dagger_{c,\downarrow}(k) c_{c,\downarrow}(k) \rangle$ (dotted black), and $n_{c,\mathrm{tot}}(k) = n_{c\downarrow}(k) + n_{c,\uparrow}(k)$ (thick blue). (Inset) For the same state, the momentum distribution on the Brillouin zone of the operators $\langle g^\dagger(k) g(k) \rangle$ (dot-dashed green), $\langle -i(f^\dagger(k) c(k) - c^\dagger(k) f(k))/2 \rangle$ (dashed orange), $\langle f^\dagger(k) f(k) \rangle$ (dotted cyan), and $\langle \hat{n}_{c_\uparrow}(k) \rangle$ (thin red). Both figures are symmetric for $k \to -k$.

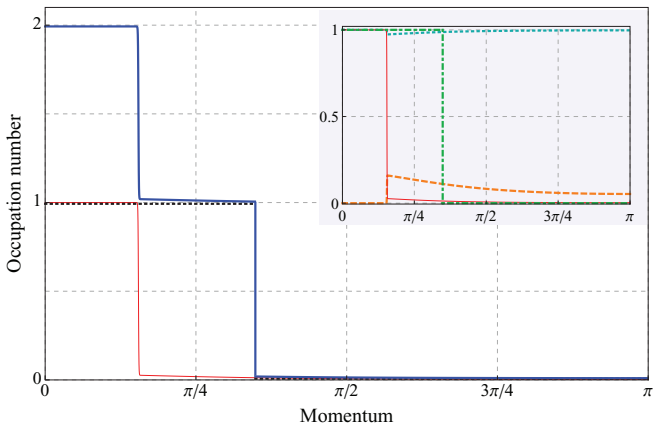

FIG. 6. (Color online) Expectation values on the FM-II cgf mean-field ground state at $x = 1.4$ and $n_c \approx 0.5$, corresponding to the band structure in Fig. 4(c). Momentum distribution on the Brillouin zone of the operators $n_{c,\uparrow}(k) = \langle c^\dagger_{c,\uparrow(k)} c_{c,\uparrow(k)} \rangle$ (thin red), $n_{c,\downarrow}(k) = \langle c^\dagger_{c,\downarrow}(k) c_{c,\downarrow}(k) \rangle$ (dotted black), and $n_{c,\mathrm{tot}}(k) = n_{c\downarrow}(k) + n_{c,\uparrow}(k)$ (thick blue). (Inset) For the same state, the momentum distribution on the Brillouin zone of the operators $\langle g^\dagger(k) g(k) \rangle$ (dotdashed green), $\langle -i(f^\dagger(k) c(k) - c^\dagger(k) f(k))/2 \rangle$ (dashed orange), $\langle f^\dagger(k) f(k) \rangle$ (dotted cyan), and $\langle \hat{n}_{c_\uparrow}(k) \rangle$ (thin red). Both figures are symmetric for $k \to -k$.

Fermi-liquid behavior, because they exist *only as components* of the coherent Kondo singlets and *not as free particles*. The only jump is visible in the majority-electron distribution (and consequently in the total distribution also). The fact that a part of the majority electrons participate in the formation of the Kondo singlets is made evident by the fact that their occupation number is not equal to one inside the Fermi volume. The position of the Fermi momentum is compatible with the picture presented, where almost all the electrons are stored in the $c_{c,\downarrow}$ (majority) band and only those that are not bounded into singlets contribute to the Fermi volume. This explains what is the nature of our mean-field solution: it separates the part of the majority-electron wave function and the spin singlets one, i.e., it stores the effective fraction of the majority electrons that can be thought as free in the g sector. The more they are, the less the Kondo singlet wave function is entangled with the majority electrons one. We want to point out how our description is not only able to move the Fermi momentum correctly, but also to renormalize the jump at the Fermi surface. This happens because the creation of the Kondo singlets spreads part of the electron-quasiparticle weight over the entire Brillouin zone. For future convenience, we also plot the momentum distribution of some cgf operators in Fig. 5 (inset). As can be seen, the hybridization takes place at every momenta, indicating that all quantum states of the minority electrons are involved into the generation of the Kondo singlets.

In the FM-I phase, the double-exchange effect clearly dominates and the Kondo effect enters as a way to optimize the energy, permitting the "annihilation" of the unwanted minority electrons, but without creating any global Kondo singlet state. In spite of that, increasing more and more the filling, the status quo does not survive up to half-filling. When a critical value $n^F_{\mathrm{crit}}(J)$ is reached, the physical properties of the system change completely, passing from the FM-I to the FM-II phase. As mentioned earlier, this happens when also the c-like band crosses the Fermi level at zero energy and starts to get filled. The filling of the c-like states is not the only thing that changes in this process. In fact, the states that get filled do not contribute anymore to the hybridization field $\mathcal{I}$, as can be seen in Fig. 6 (inset), which is an example for $x = 1.4$ and $n_c \approx 0.5$, corresponding to the band structure of Fig. 4(c). The hybridization field $I(k) = \langle -i(f^\dagger(k) c(k) - c^\dagger(k) f(k))/2 \rangle$ is zero where the $C(k) = \langle c^\dagger(k) c(k) \rangle$ is one, indicating that the filled states are well-defined $c_{c,\uparrow}$-electron states, characterized by no charge fluctuations, in contrast with the FM-I ground state where no $c_{c,\uparrow}$ state was fully occupied, because all were involved in the Kondo singlets formation.

In terms of the $c_{c,\uparrow}$ (minority) and $c_{c,\downarrow}$ (majority) electrons, what happens is that for $n_c > n^F_{\mathrm{crit}}(J)$ the system is not anymore able to keep such a high unbalance between the two electron species and tries to equilibrate the two populations. Some minority electrons escape the process of bonding into the Kondo singlets and so are allowed to hop freely from site to site. This is manifested by the creation of a Fermi surface also for the minority $c_{c,\uparrow}$ electrons, that remarkably appears in the FM-II phase, as shown in Fig. 6 for illustration purposes.

The physics of the FM-II phase is much less exotic than the one described by the FM-I phase. In fact, since the hybridization is less pronounced and both the fermion species have a Fermi surface, it is easy to relate this phase with that of an electron liquid polarized by the magnetic field generated by the impurity spins, i.e., what was previously called RKKY-ferromagnet and which corresponds to the mean-field ferromagnetic state considered in the standard literature [38]. For example, in Figs. 4(c) and 4(d), it is very evident how the c-like and g bands roughly represent the two $c_{c,\uparrow}$ and $c_{c,\downarrow}$ bands. In this scenario, the hybridization term,

remnant of the SSKI formation of the FM-I phase, optimizes the ground-state configuration incorporating the Kondo effect into it. This optimization is very efficient and in fact the FM-II phase gains a lot of energy when the coupling is increased, beating also the mean-field spiral ordered ground states [38]. The FM-II phase is related to the RKKY ferromagnetic one, in the sense that for low filling and low coupling these two kind of ground states look very much the same, becoming more and more different increasing the relevancy of the Kondo effect.

It is important to point out how the FM-II phase survives from $n^F_{\rm crit}(x)$ up to half-filling, for each $x \lesssim 2$. Of course, this does not mean that it represents the true phase of the system, and in fact it is known that the region of the phase diagram occupied by the FM-II phase is mostly paramagnetic and not ferromagnetic. It is therefore very probable that comparing the FM-II ground states with mean-field solutions that incorporate, beside the Kondo effect, also a nontranslational invariant order (i.e., the analogous of the FM-II states but with spiral order for the spins), the FM-II states would not be favorable anymore. Anyway, the numerical simulations [35] clearly indicate the existence of a ferromagnetic phase, a sort of ferromagnetic tongue, *inside* the paramagnetic dome. To the best of our knowledge, there exist no theoretical explanation for this tongue, whose ferromagnetism has never been fully understood. The FM-II states, able to dominate the spiral spin ordered trial states, provide a possible justification for the ferromagnetic tongue, and could be regarded as prototype for this kind of Kondo stabilized ferromagnetic order.

2. *Instability of the FM-I phase at intermediate couplings*

At $x \approx 2$, it appears an instability in the phase diagram. In fact, the two branches (low and high energy, mentioned at the beginning of Sec. IV A 1) of mean-field solutions collide for a critical chemical potential $\mu_{12}(x)$, corresponding to a critical density $n^{\rm pol}_{\rm crit}(x)$. This collision implies the disappearance of both the solutions, which merge into a new one: the half-filled KI. This solution is the only translationally invariant mean-field solution for $\mu^{\rm pol}_{\rm crit} < \mu^* < 0$ and it appears at $\mu^{\rm pol}_{\rm crit} > \mu_{12}(x)$ leaving an interval between $\mu_{12}(x) < \mu^* < \mu^{\rm pol}_{\rm crit}$ (shadowed region in Figs. 7 and 8) where no solution could be found. In turn, this also means that we found no solutions between $n^{\rm pol}_{\rm crit} < n_c < 1$. Although strange, this result has a quite reasonable explanation, consistent with the physics of the one-dimensional Kondo lattice.

To understand this process of collision of two solutions, one has to keep in mind the nature of the mean-field solutions, which are fixed points of our Newton-Raphson method, or also extremal points of the mean-field energy functional (see Appendix B). The only way for fixed points (or two extrema) to disappear is via a bifurcation process.

Initially, at $x \approx 2$, we found that $n^{\rm pol}_{\rm crit} \approx 1$; changing the coupling this critical density moves quickly to much smaller values, so that at $x \approx 2.2$, one has already $n^{\rm pol}_{\rm crit} \approx 0.8$. In doing this, the critical density becomes smaller than the critical density that separates the FM-I and FM-II phases, making the latter disappear from the phase diagram. So at intermediate couplings $x \gtrsim 2.1$, the FM-II phase does not exist anymore and we found only two phases: the FM-I phase between $0 < n_c < n^{\rm pol}_{\rm crit}$ and the KI phase at $n_c = 1$. We would like to point out how the value of the coupling where the FM-II phase disappears is in approximate agreement with the upper boundary of the ferromagnetic tongue phase mentioned previously, suggesting again the connection between the two phases.

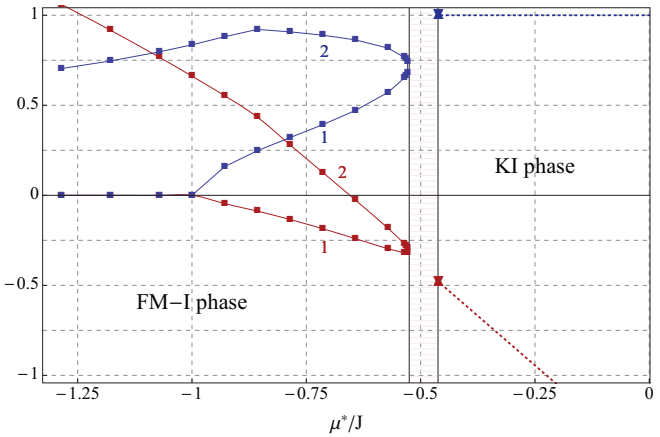

FIG. 7. (Color online) Free energy (red) and (on-site) electron density (blue) vs μ^*/J, for $x = 2.8$. On the y axis, the free energy is given in units of $4t/\pi$ and the value 0 and -1 correspond respectively to the empty and the half-filled noninteracting model; the density can vary from zero (no electrons) to one (half-filling). The labels 1 and 2 mark the low- (FM-I ground state) and high-energy mean-field solutions. The label KI indicates the half-filled Kondo insulating solution. The shaded area, delimitated by the two vertical black lines, indicates the values of the chemical potential where the bifurcation takes place. The dots of the branches 1 and 2 indicate the solutions that we found numerically, while the lines are an interpolation of the results. In the case of the KI solutions instead, we could obtain an arbitrary large amount of points, therefore the dashed KI line is drawn with machine precision. The error bars are not present, because they are smaller than the marker points.

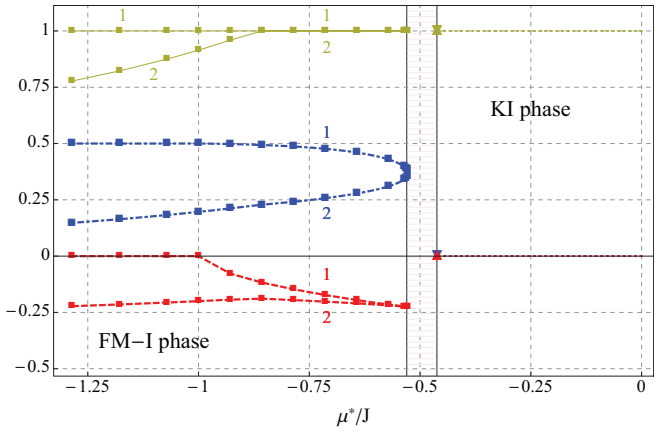

FIG. 8. (Color online) Commensurability (yellow), impurity spin magnetization $\langle S^z_f \rangle$ (blue), and electron spin magnetization $\langle c^\dagger_{c,\uparrow} c_{c,\uparrow} - c^\dagger_{c,\downarrow} c_{c,\downarrow} \rangle/2$ (red) vs μ^*/J, for $x = 2.8$. The same conventions as in Fig. 7 are used. It is evident how the commensurability is always equal on the ground state of the FM-I phase (i.e., the branch labeled by the number 1).

The absence of a solution between $n_{\rm crit}^{\rm pol} < n_c < 1$ is an annoying feature, but it hides a possible physical explanation. The picture becomes more clear analyzing the behavior of the mean-field solutions at varying chemical potentials, rather than varying density. In Fig. 7, we plot the dependence of the free energy and electron density on the chemical potential, for our mean-field solutions, choosing $x = 2.8$ for illustrative purposes (the same structure holds for all the intermediate couplings). In Fig. 8, we plot also the behavior of other physical quantities, such as the value of the commensurability parameter, impurity spin polarization and electron polarization.

On the left, the two branches of mean-field solutions can be seen. As evident, the two families become degenerate at $\mu_{12} = \mu^*/J \approx -0.53$ and converge to the same point in the parameter space, as can be understood examining the electron density curve (we reserve the symbol $\mu_{\rm crit}^{\rm pol}$ for the value of the chemical potential at which we are able to resolve the new KI phase). Increasing the chemical potential, we were not able to resolve any solution until the appearance of the KI phase at $\mu_{\rm crit}^{\rm pol}$. This is due to the fact that the mean-field energy functional becomes almost flat, making impossible the identification of maxima, minima, and flexes for values of μ^* between μ_{12} and $\mu_{\rm crit}^{\rm pol}$. The flat shape of the mean-field energy functional is the result of the collision between the two branches (fix points) and physically it has a quite natural interpretation, visible in Fig. 7. Indeed, following the ground-state branch 1, i.e., the FM-I phase, it is evident that the function $n_c(\mu^*)$ is going towards a vertical flex at μ_{12}, which also means that the derivative $dn_c(\mu^*)/d\mu^*$ diverges at μ_{12}. Since $dn_c(\mu^*)/d\mu^*$ is proportional to the compressibility [59] of the quantum liquid, its divergence signals an instability and a phase transition due to a process of phase separation. At μ_{12}, corresponding to the density $n_{\rm crit}^{\rm pol}$, the energy necessary to add an electron becomes zero. In terms of our algorithm, the divergence of the compressibility is manifested by the zero value of the Jacobian determinant, and so in the impossibility to resolve the fixed points in the shadowed region in Figs. 7 and 8.

With this in mind, we can try to explain the physics behind this behavior. As mentioned in the previous section, for small values of density (i.e., for low chemical potential), the electrons are able to delocalize on the entire lattice, creating a coherent magnetization on the entire system and generating the state FM-I that survives for higher and higher densities, stabilized by the creation of the SSKI that can be though of as a liquid of Kondo singlets. However, once the critical density $n_{\rm crit}^{\rm pol}$ is reached at μ_{12}, the FM-I is not anymore able to host new electrons and small "bubbles" of the half-filled KI phase appear in the system, separating *islands* of FM-I phases that become less and less extended increasing the total electron density. In these islands, the ferromagnetic order is still realized by the conduction electrons, via double exchange. With respect to the SSKI picture discussed previously, one understands that a qualitative two-liquid picture can be elaborated to take into account the physics of the system: in the FM-I phase below the critical density $n_{\rm crit}^{\rm pol}$, the two liquids (the majority-electrons liquid and the Kondo-singlets liquid) are homogeneously mixed on the entire lattice and their wave functions entangled. When the critical $n_{\rm crit}^{\rm pol}$ is reached, it is not energetically favorable to keep this homogeneous configuration and the two fluids separate. This phase separation is marked by the divergence of the compressibility.

This picture of the phase separated region resembles the description provided by bosonization [2,29], where the islands of coordinated spins are identified as polarons and the phase coexistence region is the polaronic liquid. In this region of the phase space, the correct degrees of freedom are [2] the islands of FM-I phase, or more properly the electrons dressed by the ferromagnetic polarized cloud of impurity spins. Our *mean-field analysis is not able to describe* the dynamics of these polarons but permits to predict their existence and locate, at intermediate couplings, their liquid phase in the correct region [35,41] of the phase diagram, although not perfectly.

Clearly, the impossibility to follow the mean-field ground state into the polaronic liquid region is a feature of our mean-field decomposition scheme (26). In principle, allowing for more hybridization channels, also an analysis of the polaronic liquid would be possible, but this would spoil the advantages of the cgf-map, making the solution very involved. It is our opinion that, if the subject of the study are the properties of the polaronic liquid, i.e., of the heavy-fermion phase of the one-dimensional Kondo lattice [2], then it would be more appropriate to modify the mapping. This unsuitability of the cgf map, as we have defined it in the mean-field description of the polaronic phase, is consistent with the fact that we optimized the mapping for the analysis of ferromagnetic (or in general translational invariantly ordered) states.

3. *The scenario at high couplings*

Increasing even more the coupling, reaching $x \gtrsim 3$, the scenario does not change, except for the fact that $n_{\rm crit}^{\rm pol}$ moves to lower and lower values. Moreover, some other unphysical mean-field solutions appear close to half-filling. We believe that these are symptoms of the fact that for such a high value of the coupling, the ground-state structure changed too much with respect to the original one. The FM-I phase stabilized by the SSKI mechanism (as we explained it previously, in the mean-field picture) does not give anymore a good approximation of the ground-state configuration. This is obviously due to the enhanced importance of the Kondo effect, which causes a stronger and stronger entanglement of the majority-electron wave-function with the Kondo-singlets one. Eventually, there is not anymore space to think of a part of the majority $c_{c,\downarrow}$ electrons as free, i.e., as a g-fermion sector completely decoupled from the c-f one, and our mean-field decomposition scheme breaks down.

Anyway, these arguments suggest the possibility for the existence of two qualitatively different ground states describing the ferromagnetic phase of the one-dimensional Kondo lattice at low and high couplings.

B. Half-filled solution: the KI state and the RKKY effect

It is well documented [1] that half-filling is a very special point for the Kondo lattice model. The configuration of the ground state is very different from the ones that are

infinitesimally close to it, in particular, for what concerns the magnetic properties of the system.

At half-filling, the system forms a spin liquid with total spin $S = 0$, characterized by a gap in both the spin and charge sector. The gaps exist for every value of the coupling, and no critical x that signals a phase transition has ever been found, although it is strongly believed that the mechanisms responsible for the existence of the gap are different in the two limits.

At small coupling, the RKKY effect causes a local antiferromagnetic [1,20] order in the impurity spins. This order is only local and quantum fluctuations destroy it at larger scales, implying the opening of the spin gap [17,21]. However, the electrons moving on the lattice feel the nearest-neighbor antiferromnagnetic order, experiencing coherent Bragg (back-)scattering and a gap opens also in the charge sector [17]. At high coupling, the nature of the gap is instead caused by the development of the local Kondo singlets. This gap is much similar to the BCS gap of superconductors [19]: it opens because a local singlet has to be broken to move the local charge or flip a local spin, costing an energy of $3J/4$. Since no phase transitions between the two regimes exists, a crossover [1] must take place around some value x.

It is quite clear that a mean-field approach will not be able to capture correctly the subtle physics of the spin liquid phase. As a matter of fact, we already tried to tackle the problem in more interesting and appropriate way [43], keeping the spin-rotational symmetry and studying the sector of nonmagnetic ground states. Anyway, a discussion of the mean-field results will not be completely meaningless, because some interesting features are correctly captured by the mean-field solutions. Moreover, it will be a good occasion to discuss the appearance of the RKKY effect in the context of the cgf map.

In our mean-field phase diagram, the particularity of the half-filled point is the existence of the KI state. Such mean-field solution exists only at half-filling, like a singular point. It is characterized by perfect [60] paramagnetism $\mathcal{F} = 1/2$ and perfect balance between the up-down population of the conduction electrons $\mathcal{C} = 1/2$. The value of the mean-field $\mathcal{I}$, which measures the average hybridization between the species c and f, is coupling dependent and goes from zero at $x \to 0$ to $1/2$ at $x \to +\infty$.

Of primary importance is the fact that $\mathcal{G} = 1$ for every value of the coupling. The fact that the g band is completely filled means that there is always one g fermion per site and therefore the available states for the description of the mean-field KI state are only (see Table I)

$$|\Downarrow\rangle, \quad |\uparrow\Downarrow\rangle, \quad |\downarrow\Uparrow\rangle, \quad |\uparrow\downarrow\Updownarrow\rangle.$$

The presence of the states with zero and two electrons seems annoying, but it is necessary in order to keep in the ground-state wave function also an uncertainty in the local conduction electron density. Indeed, only at $J \to +\infty$, when all the conduction electrons are bound into locally inert Kondo singlets, the local conduction electron density is exactly equal to one. As can be seen in Fig. 9 (inset), the mean-field KI solution is characterized by two bands (together with the flat filled g band), which come from the originally flat f band, hybridized with the originally cosine-shaped c band. The hybridization gives to the two bands the avoided-crossing

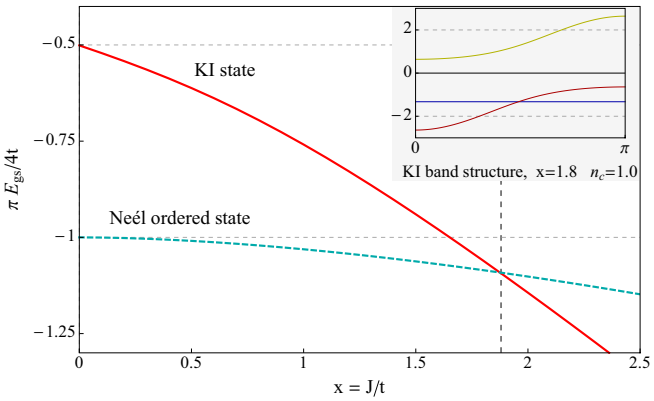

FIG. 9. (Color online) The evolution of the mean-field energy of the state KI, compared with the antiferromagnetic spin ordered ground state of Ref. [38]. (Inset) The cgf band structure of the KI ground state for the value $x = 1.8$; on the y axes, the energy is given in units of t. The same conventions of Fig. 4 have been kept; the bands are symmetric for $k \to -k$.

structure typical of Kondo insulators. This band structure does not change if the chemical potential is modified, as long as it remains inside the gap. When the critical chemical potential $\mu^{\rm pol}_{\rm crit}$ is reached, i.e., when the chemical potential level intercepts one of the bands, the KI solution collapses and a new couple of solutions (the two FM-I solutions that crush at μ_{12}) become the only mean-field solutions.

Given that $\mathcal{G} = 1$, the two bands of the half-filled KI state are found diagonalizing the $H^{\rm MFTI}_{cf}$. Defining two creation operators as

$$s^\dagger(k) = \sin(\theta_k)c^\dagger(k) + i\cos(\theta_k)f^\dagger(k),$$
$$t^\dagger(k) = \sin(\theta_k)c^\dagger(k) - i\cos(\theta_k)f^\dagger(k),$$

then the KI solution is given by the ground state

$$|KI(x)\rangle = \prod_{k=-\pi}^{\pi} s^\dagger(k)g^\dagger(k)|0_{cgf}\rangle$$
$$= \prod_{k=-\pi}^{\pi} (\sin(\theta_k)c^\dagger(k) + i\cos(\theta_k)f^\dagger(k))g^\dagger(k)|0_{cgf}\rangle, \tag{35}$$

where the x dependence enters into the functions θ_k.

For $x \to +\infty$, the KI state approaches the correct asymptotic ground state with $\mathcal{I} = 1/2$, i.e.,

$$|KI(x \to +\infty)\rangle = \prod_{k=-\pi}^{\pi} \frac{1}{\sqrt{2}}(c^\dagger(k) + if^\dagger(k))g^\dagger(k)|0_{cgf}\rangle.$$

The fact that $|KI\rangle$ is the correct mean-field ground state for $x \to +\infty$ can be understood also without any numerical analysis looking at $H^{\rm MFTI}_{cgf}$ putting $t = 0$ and sending J to infinity. Approaching the correct infinite-coupling ground state, it is not surprising that also the correct asymptotic energy density dependence of $-3x/4$ is recovered.

It is important to note that in this limit, the ground state is correctly given by a linear combination of Kondo singlets: one for each site. In fact, on each site, one has the realization

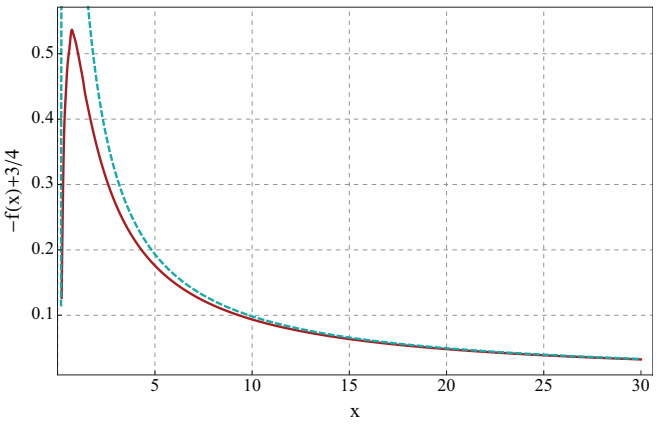

FIG. 10. (Color online) The different curves are the numerically determined $f(x) = \mu^{\rm pol}_{\rm crit}(x)/J$ (solid red) and $f(x) = \Delta_{qp}(x)/J = 1/6x^2 - 1/x + 3/4$, (dashed blue) that is the perturbative $t/J = 1/x$ expansion for the quasiparticle gap.

of the state $s^\dagger g^\dagger|0\rangle$ that means $(c^\dagger + if^\dagger)g^\dagger|0\rangle$ that by the cgf map Table I is $|\uparrow\Downarrow\rangle - |\downarrow\Uparrow\rangle$. In the case $x < +\infty$, the k dependence of θ_k spoils the singlets with components coming form the states $|\Downarrow\rangle$ and $|\uparrow\downarrow\Uparrow\rangle$, necessary to take into account the hopping of the electrons; while the fact that $\theta_k \neq \pi/4$ implies also the contribution of the triplet component with spin $S^z_{\rm tot} = 0$. These properties are in agreement with the known high coupling solutions [18,19].

The mean-field gap between the two bands, which corresponds at infinite coupling to the gap between the singlet and triplet states at $S^{\rm tot}_z = 0$, is equal to $3x/2$. Unfortunately, this mean-field gap does not agree with the correct spin-gap of the Kondo insulator solution, which should be equal to x in the high coupling limit. However, this is not so surprising, because one cannot expect to predict properties of the excited states using a trivial (time-independent) mean-field theory. By construction, the critical chemical potential $\mu^{\rm pol}_{\rm crit}$ corresponds to the energy necessary to add or remove one particle from the system. This energy has been already defined in the KLM as the quasiparticle gap; we compare the value of $\mu^{\rm pol}_{\rm crit}$ and of the quasiparticle gap, using the known [1] high coupling perturbative expansion to compute it. As evident in Fig. 10, the asymptotic behavior at high coupling is the same. Anyway, around $x \approx 10$, a qualitative change in the behavior of the gap is expected [1], due to the non-negligible effect of the RKKY interaction, therefore both the curves are not relevant below that value of the coupling. The inadequacy of the state $|{\rm KI}(x)\rangle$ at small coupling is made evident by the fact that for $x \lesssim 2$ it is neither the energetically most favorable solution among the translationally invariant ones, because also the FM-II phase exists at half-filling. An analysis of (34) immediately reveals the problem: at small x, clearly the system prefers the strongly ferromagnetic order to the paramagnetic one because the kinetic energy contribution of the g fermions gets maximized (recall that in the FM-II phase, the g fermions can be interpreted as the $c_{c,\downarrow}$ electrons). So as long as one considers only translationally invariant solutions, the ferromagnetic order at small coupling is not avoidable.

However, if one instead looks at (28), it becomes clear that there exist a way to recover the kinetic energy of the g fermions, without implying ferromagnetic ordering of the impurity spins. In fact, assuming (perfect) *antiferromagnetic* order, one obtains for H_g:

$$H_g^{\rm AF} = t(1-2\mathcal{F})\sum_n (g^\dagger \tilde{g}^\dagger + \tilde{g} g) + \frac{J}{4}(-1-4\mathcal{I})\sum_n g^\dagger g,$$

where $\mathcal{F}$ is the mean-field on the first site of the double unit cell and we assumed $\mathcal{I} = {\rm const}$ for sake of simplicity. This Hamiltonian can be solved in many ways, for example, doubling the unit cell, mapping $\tilde{g} \to a^\dagger$ and making use of Nambu spinors. It is clear that the contribution from the kinetic energy is equally well obtained, and so this state will approach the energy value of the half-filled zero-coupling solution as well as the ferromagnetic one. This can also be understood using (11): assuming saturated impurity spin ferromagnetism then the g-fermion operators are the $c_{c,\downarrow}$ operators and $g^\dagger = c^\dagger_{c,\downarrow}$; assuming instead saturated spin antiferromagnetism we have $g^\dagger = c^\dagger_{c,\downarrow}$ on the sites with spin up and $g^\dagger = c_{c,\downarrow}$ on the sites with spin down. Therefore the hopping term $g^\dagger \tilde{g}^\dagger$ in the antiferromagnetic case is exactly $c^\dagger_{c,\downarrow}\tilde{c}_{c,\downarrow}$.

To study the competition of the antiferromagnetic and the ferromagnetic ground states, we should solve the mean-field Hamiltonian (34) imposing translational invariance on the doubled unit cell. This is not the analysis that we carried on.

The imposition of perfect antiferromagnetism, i.e., $\mathcal{F}_{n+1} = 1 - \mathcal{F}_n$ with $\mathcal{F}_n = 0$, implies that no hybridization is possible between the c and the f fermions (otherwise, the value of the $\mathcal{F}$ field would be spoiled), hence $\mathcal{I} = 0$. This also means that all the interesting features of our model are neglected, as the Kondo effect, and only the RKKY effect is kept into consideration. The solution for the energy of the antiferromagnetic ground state at half-filling is the well known [38]:

$$E_{\rm AF}(x) = -\frac{1}{\pi}\int_0^\pi \sqrt{\frac{x^2}{16} + 4\sin^2(k)}dk. \qquad (36)$$

It is evident that the Hamiltonian (28) contains all this physics, and therefore its study (without forcing perfect antiferromagnetism) will improve this RKKY-focused description. In particular, it will permit to study how the Kondo effect and the RKKY effect relate to each other. However, it is our opinion that other paths, rather than the mean-field analysis, could also be followed; see Refs. [40,43], for examples of such a study. Indeed, at half-filling, the most important feature that should be captured is the global singlet nature of the ground state; a feature that would be completely lost in any mean-field analysis that breaks translational invariance. Moreover, away from half-filling, the incommensurability of the order would imply an increase of the unit cell used, bringing quickly to an untreatable form for the mean-field problem.

For all these reasons and because the focus of the present work is on the ferromagnetism in the one-dimensional KLM, we will not analyze these cases, but we will use the known results of the Neél ordered ground state to make a comparison and complete our analysis. As can be seen in Fig. 9, the KI

state has a better energy, with respect to the antiferromagnetic ordered state, already at $x \approx 1.9$.

V. CONCLUSIONS AND OUTLOOK

In this paper, we have introduced an alternative representation of the Kondo lattice model, in terms of three spinless fermions interacting on a lattice. The identification of this map demonstrates by direct inspection the known [40] representation of the KLM in terms of six Majorana fermions; moreover, it generates a Hamiltonian that is very suitable for the analysis of ferromagnetism in the one-dimensional Kondo lattice.

We performed such an analysis and showed how, already at mean-field level, many properties of the phase diagram could be detected and explained. This is made possible by the identification of a symmetry of the Hamiltonian that is responsible for the appearance of the "commensurability parameter."

Our work considerably improves the available mean-field analyses and is consistent with some recent results obtained [41] by DMRG calculations, on the nature of the ferromagnetic metallic phase at intermediate and low couplings. In particular, we find the same value for the commensurability parameter and identify the same description of the system in terms of "minority" and "majority" electrons, together with the emergence of the spin-selective Kondo insulator (SSKI), reported in recent studies [41].

We showed how the existence of the SSKI stabilizes the ferromagnetic FM-I phase in the low density sector of the phase diagram. At couplings $x \lesssim 2$, the system is in the FM-I phase only for densities $n_c < n^F_{\rm crit}(x)$, while it is in the FM-II phase for $n^F_{\rm crit}(x) < n_c < 1$.

The phase transition line $n^F_{\rm crit}(x)$ lies reasonably close to the ferromagnetic-paramagnetic transition line, signaling correctly the instability of the SSKI mechanism for excessively high densities. The FM-II phase, which takes over beyond this transition, was instead identified as a solution related to the RKKY-ferromagnetic one, but optimized in order to capture more of the Kondo physics. This phase is present in the region of the phase diagram typically occupied by paramagnetic ground states, for $x \lesssim 2$. At low coupling, it is energetically more competitive than the usual mean-field states with spiral spin order. This means that our result could, in principle, be further improved considering modulations of the mean fields. Existing up to half-filling and for any coupling $x \lesssim 2$, the FM-II phase represents a valid prototype for the ferromagnetic tongue phase [35] that exists inside the ferromagnetic dome. To the best of our knowledge, there exist no other (not fully numerical) approach able to justify the existence of a ferromagnetic phase in correspondence of the ferromagnetic tongue.

At coupling larger than $x \approx 2$, the FM-II phase disappears and a region of phase coexistence between the FM-I phase and the half-filled Kondo insulating one appears. We believe that such a region is due to the failure of the hypothesis done in the mean-field decomposition of the Hamiltonian. However, the physical picture described by our results is not in contrast with the known physics of the KLM. Moreover, it suggests a qualitative change in the properties of the ferromagnet for high couplings.

At half-filling, we discovered another translational invariant solution (that exists as a singular point in the phase diagram). We identify this solution with the Kondo insulating one, recognizing that asymptotically it converges to the correct ground state, with the correct coupling dependence for the energy of the ground state and for the quasiparticle gap. However, for small couplings, it is not a good trial ground state. We do not accomplish in this manuscript any detailed analysis of the half-filled solutions, which instead have been the subject of a different study. In the present work, we simply identify the relation between the usual spiral ordered approximate solutions and our own.

Considered the great amount of physics, and the qualitatively convenient pictures that we have been able to elaborate, we hope to have demonstrated to the reader the convenience of the analysis of the KLM in terms of Majorana fermions. In this work, we used the Majoranas to identify the three spinless fermions c, g, and f. We believe that the Majorana map is, in general, very advantageous for the definition of these kind of nonlinear fermion-spin mappings. A generalization of our approach, if appropriately used, can open the doors towards a convenient description of a huge amount of unknown phenomena.

As final remark, we would like to remind the reader that the cgf map holds in any number of dimension. Therefore differently from bosonization or DMRG that find little use away from one dimension, our analysis can be straightforwardly applied also in two and three dimensions.

ACKNOWLEDGMENT

We wish to thank the Swedish research council (Vetenskapsrådet) for funding.

APPENDIX A: FERMION REPRESENTATION

It is well known that in many condensed matter systems the electron does not behave as an elementary degree of freedom. In recent years, it became evident, both from theoretical and experimental points of view, that under specific circumstances, the collective electron modes, describing a normal Fermi liquid, can decompose into more fundamental excitations with different quantum numbers and statistics [61], e.g., [62] spinons, holons, and orbitons. The development of a formalism that does not focus on the quantum numbers of the electron and puts aside its elementary nature could therefore be conceptually and formally advantageous. It is our opinion that the best candidate for such a more elementary formalism is given by the Majorana representation of the quantum degrees of freedom.

Using *nonlinear transformations* [63] on the local Fock space, it becomes straightforward to represent the fermion creation/annihilation operators of a spinful electron in terms of *composite holon-spin operators* [44]. The analysis of this kind of transformations turns out to be quite natural in terms of Majorana fermions [45]. A comprehensive discussion on these aspects will be the subject of another study [50], so in this Appendix, we outline some known practical results

that have been already used in the analysis of the Hubbard model [44,45,63] and that will be useful in our main discussion.

In the literature on Majorana fermions, the most used representation of spinful electron operators is given by (3) and (4). Another equivalent one [45] is

$$c_\uparrow^\dagger = -\sqrt{2}\Phi\sigma^+, \tag{A1}$$

$$c_\downarrow^\dagger = \frac{2\Phi\sigma_z + i\Psi}{\sqrt{2}}, \tag{A2}$$

where Φ, Ψ are Majoranas and $\sigma^+ = (\sigma_x + i\sigma_y)$, $\sigma^- = (\sigma_x - i\sigma_y)$ and σ_z are the usual Pauli operators, with the convention $\sigma_z^2 = 1/4$. The relation between (3) and (4) and (A1) and (A2) is given by the identifications

$$\Phi = 2i\gamma_1\gamma_2\gamma_3, \qquad \Psi = \gamma_4, \tag{A3}$$

$$\sigma^x = -i\gamma_2\gamma_3, \quad \sigma^y = -i\gamma_3\gamma_1, \quad \sigma^z = -i\gamma_1\gamma_2. \tag{A4}$$

This representation for the creation/annihilation operators of the spinful electron realizes the decomposition of the electron into its spinonic and holonic components [44,45], given respectively by the three Pauli operators σ_i and by the spinless fermion with creation operator $h^\dagger = (\Phi + i\Psi)/\sqrt{2}$. With these definitions, it is possible to see that there exists a one-to-one correspondence between the Hilbert space generated by the operators (3) and (4) starting from the vacuum state $|0\rangle$ such that $c_\downarrow|0\rangle = c_\uparrow|0\rangle = 0$, and the Hilbert space generated by the operators $\{1,h\} \otimes \{\sigma^+,\sigma^-\}$ and their hermitian conjugates, where $h|0_h\rangle = 0$ and $\sigma^+|\Uparrow\rangle = \sigma^-|\Downarrow\rangle = 0$. The mapping is given schematically in Table II.

Two comments are in order on the operators $h^\dagger$ and σ. First of all, it is remarkable that the Pauli operators (A4) have to be interpreted as spin or (charge) pseudospin operators, depending upon the presence or the absence of the holon associated to $h^\dagger$. Secondly, it is appropriate to note that the spinless-fermion creation operator $h^\dagger$ is obtained via a transformation that mixes the original Majorana γ_4 with the composite Majorana $2i\gamma_1\gamma_2\gamma_3$. This gives an immediate understanding of the connection between the Hilbert space of the 1-site Anderson model and the Hilbert space of the one-site Kondo lattice model described in Sec. II: in fact the confining term $U(n_f - 1)^2$ is easily rewritten as $U(1 - \phi^\dagger\phi)$, where ϕ is the holon associated to the spinful electron described by $f^\dagger$ in (2). Consequently, also the origin of the operators (6) becomes clear: for $U \to +\infty$ there must be one holon ϕ per site, that means one spinful f electron per site; therefore the operators (6) must be interpreted as the spin operators of the original f electron.

TABLE II. Mapping, as introduced in Ref. [45], between the two different representations of the Hilbert space associated with a local spinful electron. On the left, the spinor representation, given by the operators $c_\downarrow$, $c_\uparrow$, and Hermitian conjugates; on the right, the representation given in terms of holon and Pauli operators.

$\|0\rangle$	$\longleftrightarrow$	$\|0_h\rangle \otimes \|\Downarrow\rangle$
$\|\uparrow\downarrow\rangle$	$\longleftrightarrow$	$\|0_h\rangle \otimes \|\Uparrow\rangle$
$\|\uparrow\rangle$	$\longleftrightarrow$	$\|1_h\rangle \otimes \|\Uparrow\rangle$
$\|\downarrow\rangle$	$\longleftrightarrow$	$\|1_h\rangle \otimes \|\Downarrow\rangle$

APPENDIX B: GENERALIZED ALGORITHM FOR MEAN-FIELD ANALYSIS OF NONQUADRATIC HAMILTONIANS

We outline the numerical procedure that we have used to study our system. The method is not original [64] but being unpublished it requires a quick (although not complete) introduction.

Mean-field theories are variational theories where the variational parameters are the mean fields (order parameters) and the Hilbert space is given by the states that can be written as a single Slater determinant of *properly defined* one-particle states. The quantity that has to be minimized is the free energy. In particular, a well-known theorem [65] says that

$$F_{\text{true}} \leqslant F_{\text{trial}}, \tag{B1}$$

where F_{true} is the free energy associated to the density matrix of the original Hamiltonian H. A mean-field solution extremizes the function F_{trial}, with respect to small variations of the mean-field parameters.

Since the mean-field result is expressible as a Slater determinant, it means that there must exist a quadratic Hamiltonian $\tilde{H}_{\text{mf}}$ generating the mean-field one-particle states; consequently, there must exist a mean-field density matrix $\tilde{\rho}_{\text{mf}} = \exp(-\beta\tilde{H}_{\text{mf}})/\tilde{Z}$, so that

$$F_{\text{trial}} = \text{Tr}\,(\tilde{\rho}_{\text{mf}} H) - T S_{\tilde{\rho}_{\text{mf}}}. \tag{B2}$$

In second quantization terms, this Hamiltonian must take the form

$$\tilde{H}_{\text{mf}} = \sum_i \mu_i A_i, \tag{B3}$$

where the μ_i are (real) parameters that we call *variational parameters* and the A_i are *all* the possible quadratic (Hermitian) operators, written in terms of the original particle creation/annihilation operators that appear in H. For future convenience, the parameters $\alpha_i = \langle A_i\rangle = \text{Tr}(\tilde{\rho}_{\text{mf}} A_i)$ are named *order parameters*. It is evident that the specific value of any order parameter α_j will (in general) depend on the entire set $\{\mu_i\}$.

This means that the term $\text{Tr}\,(\tilde{\rho}_{\text{mf}} H)$ will correspond to the mean-field energy functional that one can obtain via Wick decomposition of all the operators that belong to H. So

$$\langle H\rangle = \text{Tr}(\tilde{\rho}_{\text{mf}} H) = \mathcal{H}(\alpha_i), \tag{B4}$$

which implicitly means also $\mathcal{H}(\mu_i)$. Of course, the same can be said for the term $T S_{\tilde{\rho}_{\text{mf}}}$ that becomes $T\mathcal{S}(\mu_i)$.

The best mean-field solution is given by the density matrix that minimizes (B1), but in general all the solutions that extremize it are acceptable mean-field solutions. Of course, the best one will be the one with the lowest free energy. Extremizing $F_{\text{trial}}(\mu_i) = \mathcal{H}(\mu_i) - T\mathcal{S}(\mu_i)$, one obtains the condition

$$0 = \left(\frac{\partial\mathcal{H}}{\partial\alpha_i} - \mu_i\right)\frac{\partial\alpha_i}{\partial\mu_j}. \tag{B5}$$

Unless it happens that there exists an α_i independent of all the $\{\mu_j\}$, then one must have

$$\frac{\partial \mathcal{H}}{\partial \alpha_i} = \mu_i. \tag{B6}$$

This is a set of (nonlinear) equations in the parameters $\{\mu_i\}$; clearly, there exists one equation per μ_i.

The algorithm is then implemented in a straightforward way. (1) Given the original Hamiltonian H, one has to start writing down all the possible (not necessarily Hermitian) pairings of creation/annihilation operators that appear in H, generating a set of possible order parameters β_i (note that this set can be infinite in principle, because it can contain also very nonlocal order parameters). An analysis of the set $\{\beta_i\}$ must be done, inserting the information about the physics: for example, symmetries, continuous or discrete, that have to be preserved (for example, translational invariance, or time-reversal symmetry) or conditions given by the Hermitian character of the Hamiltonian (for example, if $\langle c^\dagger g^\dagger \rangle = \Delta$ then $\langle cg \rangle = -\Delta^*$ by Hermiticity). This will create the set of order parameters $\{\alpha_i\}$, in general smaller (always finite), introduced previously.

(2) Given the many order parameters α_i, one writes down the operators A_i that correspond to them, such that $\langle A_i \rangle = \alpha_i$. Note that these operators can be (properly normalized) linear combinations of quadratic operators.

(3) Given H and the set $\{\alpha_i\}$, one can write down the mean-field functional $\mathcal{H}(\alpha_i)$ obtained by the standard Wick decomposition.

(4) Using (B6) one writes down the (nonlinear) system in terms of the variation parameters μ_i. This nonlinear system can then be solved numerically, and its solutions are by construction also mean-field solutions of the Hamiltonian H.

Although there are some physical interesting features hidden in this method, we are not going to comment on it further here. The method, treating all the mean-fields on equal footing, proved itself quite good in the study of the competition between different order parameters.

[1] H. Tsunetsugu, M. Sigrist, and K. Ueda, Rev. Mod. Phys. **69**, 809 (1997).
[2] M. Gulácsi, Adv. Phys. **53**, 769 (2004).
[3] M. Gulácsi, Philos. Mag. **86**, 1907 (2006).
[4] A. C. Hewson, *The Kondo Problem to Heavy Fermions* (Cambridge Universtiy Press, Cambridge, UK, 1993).
[5] P. Nozières, J. Phys. Soc. Jpn. **74**, 4 (2005).
[6] S. Burdin, A. Georges, and D. R. Grempel, Phys. Rev. Lett. **85**, 1048 (2000).
[7] D. Meyer and W. Nolting, Phys. Rev. B **61**, 13465 (2000).
[8] P. Fazekas, *Lecture Notes on Electron Correlation and Magnetism* (World Scientific, Singapore, 1999).
[9] K. Yosida, Phys. Rev. **106**, 893 (1957).
[10] M. A. Ruderman and C. Kittel, Phys. Rev. **96**, 99 (1954).
[11] P. W. Anderson and H. Hasegawa, Phys. Rev. **100**, 675 (1955).
[12] C. Zener, Phys. Rev. **81**, 440 (1951).
[13] P. G. de Gennes, Phys. Rev. **118**, 141 (1960).
[14] P. Coleman, Phys. Rev. B **28**, 5255 (1983).
[15] P. Coleman, in *Handbook of Magnetism and Advanced Magnetic Materials*, edited by H. Kronmuller and S. Parkin (Wiley, 2007), Vol. 1, pp. 95–148.
[16] K. Ueda, Physica B: Condens. Matter **230-232**, 22 (1997).
[17] K. Le Hur, Phys. Rev. B **58**, 10261 (1998).
[18] R. Eder, O. Rogojanu, and G. A. Sawatzky, Phys. Rev. B **58**, 7599 (1998).
[19] R. Eder, O. Stoica, and G. A. Sawatzky, Phys. Rev. B **55**, R6109 (1997).
[20] G.-S. Tian, Phys. Rev. B **50**, 6246 (1994).
[21] A. M. Tsvelik, Phys. Rev. Lett. **72**, 1048 (1994).
[22] O. Bodensiek, R. Zitko, M. Vojta, M. Jarrell, and T. Pruschke, Phys. Rev. Lett. **110**, 146406 (2013).
[23] M. Z. Asadzadeh, F. Becca, and M. Fabrizio, Phys. Rev. B **87**, 205144 (2013).
[24] E. S. Sørensen, M.-S. Chang, N. Laflorencie, and I. Affleck, J. Stat. Mech. (2007) L01001; E. Eriksson and H. Johannesson, Phys. Rev. B **84**, 041107 (2011).
[25] K. Ueda, T. Nishino, and H. Tsunetsugu, Phys. Rev. B **50**, 612 (1994); P. Coleman, C. Pépin, Q. Si, and R. Ramazashvili, J. Phys.: Condens. Matter **13**, R723 (2001); T. Senthil, S. Sachdev, and M. Vojta, Phys. Rev. Lett. **90**, 216403 (2003); H. v. Löhneysen, A. Rosch, M. Vojta, and P. Wölfle, Rev. Mod. Phys. **79**, 1015 (2007); A. Tsvelik and M. Oshikawa, *New Theoretical Approaches to Strongly Correlated Systems*, NATO Science Series (Springer, Netherlands, 2001), Vol. 23, pp. 117–137; M. Yamanaka, M. Oshikawa, and I. Affleck, Phys. Rev. Lett. **79**, 1110 (1997).
[26] M. Sigrist, H. Tsunetsugu, and K. Ueda, Phys. Rev. Lett. **67**, 2211 (1991).
[27] C. Lacroix, Solid State Commun. **54**, 991 (1985).
[28] M. Sigrist, H. Tsunetsugu, K. Ueda, and T. M. Rice, Phys. Rev. B **46**, 13838 (1992).
[29] G. Honner and M. Gulácsi, Phys. Rev. Lett. **78**, 2180 (1997).
[30] K. Le Hur, Phys. Rev. B **62**, 4408 (2000).
[31] S. Fujimoto and N. Kawakami, J. Phys. Soc. Jpn. **63**, 4322 (1994).
[32] C. C. Yu and S. R. White, Phys. Rev. Lett. **71**, 3866 (1993).
[33] M. Troyer and D. Würtz, Phys. Rev. B **47**, 2886 (1993).
[34] N. Shibata and K. Ueda, J. Phys.: Condens. Matter **11**, R1 (1999).
[35] I. P. McCulloch, A. Juozapavicius, A. Rosengren, and M. Gulacsi, Phys. Rev. B **65**, 052410 (2002).
[36] I. Hagymási, K. Itai, and J. Sólyom, Phys. Rev. B **85**, 235116 (2012).
[37] C. Lacroix and M. Cyrot, Phys. Rev. B **20**, 1969 (1979).
[38] P. Fazekas and E. Müller-Hartmann, Zeitschrift für Physik B **85**, 285 (1991).
[39] J. R. Schrieffer and P. A. Wolff, Phys. Rev. **149**, 491 (1966). Phys. Rev. B **65**, 212303 (2002).
[40] J. Nilsson, Phys. Rev. B **83**, 235103 (2011).
[41] R. Peters and N. Kawakami, Phys. Rev. B **86**, 165107 (2012).
[42] R. Peters, N. Kawakami, and T. Pruschke, Phys. Rev. Lett. **108**, 086402 (2012).
[43] J. Nilsson and M. Bazzanella, Phys. Rev. B **88**, 045112 (2013).

[44] S. Östlund and M. Granath, Phys. Rev. Lett. **96**, 066404 (2006).
[45] B. Kumar, Phys. Rev. B **77**, 205115 (2008).
[46] S. Östlund, Phys. Rev. B **76**, 153101 (2007).
[47] P. Coleman, E. Miranda, and A. Tsvelik, Phys. Rev. Lett. **70**, 2960 (1993).
[48] P. Coleman, L. B. Ioffe, and A. M. Tsvelik, Phys. Rev. B **52**, 6611 (1995).
[49] B. S. Shastry and D. Sen, Phys. Rev. B **55**, 2988 (1997).
[50] M. Bazzanella and J. Nilsson (unpublished).
[51] C. S. Hellberg and E. J. Mele, Phys. Rev. Lett. **67**, 2080 (1991); Phys. Rev. B **44**, 1360 (1991).
[52] The operator $A_3 = \sum_n A_3(n)$ commutes with the Hamiltonian for any value of the chemical potential μ^*. For the particular value $\mu^* = 0$, also two other operators A_1 and A_2, with form similar to A_3, can be found.
[53] S. Sachdev, *Quantum Phase Transitions* (Cambridge Universtiy Press, Cambridge, UK, 1999).
[54] A. Kitaev and C. Laumann, in *Exact Methods in Low-Dimensional Statistical Physics and Quantum Computing*, Lecture Notes of the Les Houches Summer School, Vol. 89, 2008 (Oxford University Press, 2009), pp. 101–125.
[55] We accepted only the solutions that were able to solve the nonlinear system within a better accuracy than 10^{-12}.
[56] A. Juozapavicius, I. P. McCulloch, M. Gulacsi, and A. Rosengren, Philos. Mag. Part B **82**, 1211 (2002).
[57] I. M. Lifshitz, Sov. Phys. JETP **11**, 1130 (1960). Y. M. Blanter *et al.*, Phys. Rep. **245**, 159 (1994).
[58] The mean-field could also take value 0, with all the spins pointing down and implying the reversing of the g band. This is not in contradiction with the results, and it is a simple feature of the choice of the map. In fact, such an inversion corresponds to the simultaneous application of a parity transformation for the spin polarization axis and a particle-hole transformation in the down-electron band. Therefore the g fermions will not describe electrons propagating in an empty band, but holes in a filled one. It is clear that the same physical picture is recovered, although it is expressed in very complicated terms. In the cgf map, the choice of the direction of the impurity spins determines also a choice in how the charge of the electrons with opposite spin is counted.
[59] P. Nozières and D. Pines, *The Teory of Quantum Liquids* (Perseus Books, 1999).
[60] Within our numerical precision, in this case is fixed arbitrarily in 10^{-9}.
[61] B. J. Kim *et al.*, Nat. Phys. **2**, 397 (2006); Y. Chen, D. Förster, and A. Larkin, Phys. Rev. B **46**, 5370 (1992); J. Schlappa *et al.*, Nature (London) **485**, 82 (2011); H. F. Pen, J. van den Brink, D. I. Khomskii, and G. A. Sawatzky, Phys. Rev. Lett. **78**, 1323 (1997); T. Shimojima *et al.*, Science **332**, 564 (2011).
[62] In this list, we could include also the theoretically predicted pure Majorana excitations, but with an experimental decisive result being still absent, we omit them.
[63] S. Östlund and E. Mele, Phys. Rev. B **44**, 12413 (1991).
[64] Stellan Östlund (unpublished).
[65] R. Feynman, *Statistical Mechanics, a Set of Lectures* (W.A. Benjamin Inc, 1965).